



Recent Advances in First-Row Transition Metal/Chiral Phosphoric Acid Combined Catalysis

Gui-Chun Fang¹ · Yong-Feng Cheng¹ · Zhang-Long Yu¹ · Zhong-Liang Li² · Xin-Yuan Liu¹

Received: 29 April 2019 / Accepted: 16 August 2019
© Springer Nature Switzerland AG 2019

Abstract

Since the pioneering independent reports of Akiyama and Terada, the use of chiral phosphoric acids (CPAs) and derivatives as a versatile tool for asymmetric synthesis with good reactivity, regioselectivity, diastereoselectivity and enantioselectivity has emerged, forming an important part of the implementation of asymmetric counteranion-directed catalysis reported to date. In these achievements, the combination of metals with CPAs has enabled various catalytic modes beyond the scope of typical acid catalysis, such as relay catalysis, ion-pairing catalysis, and binary acid catalysis. The first-row transition metals (Sc–Zn) are considered to be sustainable transition metals and have received a great deal of attention. These naturally abundant metals display excellent Lewis acidity and function as powerful redox catalysts in synthesis involving both one and two-electron transfers. Hence, in this chapter, we summarize recent advances in the development of asymmetric reactions using a combination of first-row transition metals and CPAs. Furthermore, we provide a detailed discussion of the mechanisms involved in order to understand the interaction of the metal/phosphate and the origins of the asymmetric control of the transformations.

Keywords Asymmetric catalysis · First-row transition metals · Chiral phosphoric acids · Relay catalysis · Binary-acid catalysis · Enantioselectivity

This article is part of the Topical Collection “Asymmetric Organocatalysis Combined with Metal Catalysis”, edited by Bruce A. Arndtsen, Liu-Zhu Gong.

✉ Xin-Yuan Liu
liuxy3@sustech.edu.cn

¹ Department of Chemistry and Shenzhen Grubbs Institute, Southern University of Science and Technology, Shenzhen 518055, China

² SUSTech Academy for Advanced Interdisciplinary Studies, Southern University of Science and Technology, Shenzhen 518055, China

1 Introduction

Chiral Brønsted acids, in particular 1,1'-bi-2-naphthol (BINOL)-derived phosphoric acids, have emerged as an increasingly prominent tool for asymmetric synthesis [1, 2]. The chiral phosphoric acids (CPAs, Fig. 1) containing acid/base dual function simultaneously, have been widely recognized as effective organocatalysts [3–5], and significant progress has been made in their utilization since the seminal reports by the groups of Akiyama [6] and Terada [7] individually in 2004 [8–11]. Besides BINOLs, chiral diols bearing C₂-symmetry, e.g., H₈-BINOL, SPINOL, VAPOL, VANOL, and TADDOL, have been used as variants of CPAs [5]. The majority of catalyst modifications for CPAs aim towards tuning the substituents at the 3,3'-positions of binaphthyl skeletons to achieve high selectivity. A new family of planar CPAs has also been reported recently, including ferrocene-bridged paracyclophane [12–15] and 1,8-biphenylene-tethered paracyclophane [16] frameworks.

In view of their application as chirality-inducing agents, CPAs conventionally provide hydrogen-bonding interactions to form a contact ion pair with electrophilic components, through their relatively strong, yet appropriate, acidity [17, 18]. Further, the combination of metals and CPAs has exhibited multiple and peculiar reactivity beyond the single acid effect for asymmetric reactions, and many review articles covering this area have been published [19–32]. Up to now, various transition-metals such as Pd [33–35], Ag [4, 36, 37], Rh [38–40], Ir [41–43], Au [44–47], Ru [48–51], Fe [52], Cu [53, 54], and main metals e.g., Mg [55–57], Ca [58–60], and In [61, 62], have been employed in such dual catalytic systems. According to literature reports and catalytic principles, these systems are generally divided into four catalytic modes: relay catalysis (or cascade catalysis, sequential catalysis, Fig. 2a), counteranion-directed catalysis (CDC) (Fig. 2b) [27, 29, 47], chiral phosphate catalysis (Fig. 2c), and binary-acid catalysis (Fig. 2d) [19–24, 26, 32]. The resulting ion-pairing between the chiral anion (i.e., phosphate anion) and cationic metal complex (Fig. 2b), or metal cation (Fig. 2c) allows high efficiency and stereocontrol of the reactions [29]. In the binary-acid catalysis [32], the free phosphoric acid serves as a dual neutral ligand and Brønsted acid catalyst, resulting in a single binary complex bearing a bi-/multi-activation site (e.g., proton and metal center). The counter anion or ligand in the metal cation also shows a dramatic effect on catalytic performance. Besides protons, a second metal species, such as lithium and calcium, etc., can also have a synergistic effect in catalysis.

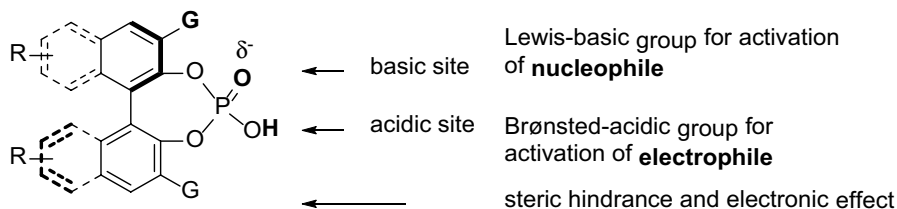


Fig. 1 Chiral phosphoric acid (CPA) analogs

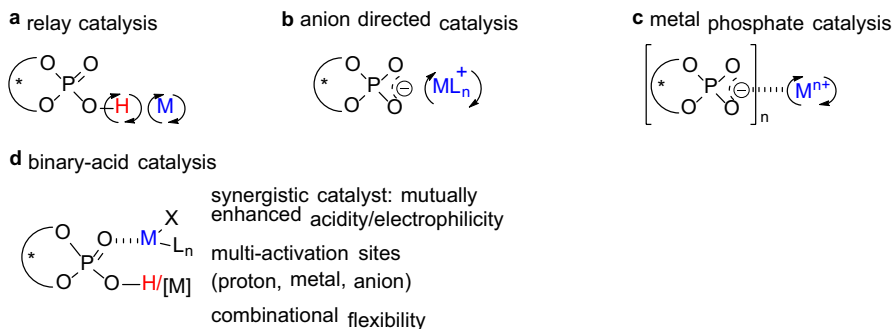


Fig. 2a–d Catalytic modes combining phosphoric acids and metals. **a** Relay catalysis, **b** anion-directed catalysis, **c** metal phosphate catalysis, **d** binary-acid catalysis

Among the wide range of transition metals, first-row transition metals (Sc–Zn) display unique advantages (Fig. 3), such as affordability, less toxicity, environment-friendliness, and abundance, ranging from 16 ppm (Sc) to 43,200 ppm (Fe) in the Earth’s continental crust [63–70]. Further, these metal complexes have proven to be powerful Lewis acid catalysts, as well as redox catalysts for reactions via either one- or two-electron transfers [66, 71]. For example, copper [72, 73] and nickel [74–77] have been well established as single-electron transfer (SET) catalysts to initiate radical reactions. Based on a statistical analysis of the literature, the combination of first-row transition metals (Mn, Fe, Cu, Zn, etc.) with CPAs has received continuous attention and great progress has been made in this field in recent years. In this current review, we summarize recent advances in catalytic asymmetric reactions promoted by the combination of first-row transition metals with CPAs (Fig. 3). According to the metal catalysis involved, the content is divided into six sections, consisting of Mn, Fe, Cu, Zn, Sc and miscellaneous metals with CPAs.

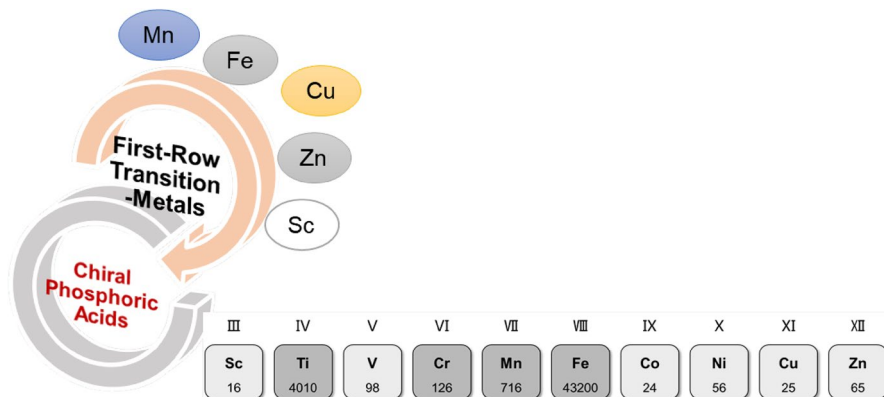


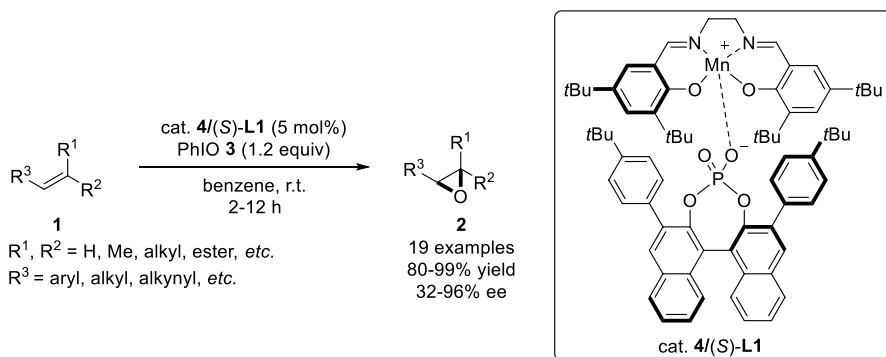
Fig. 3 Combining first-row transition-metals and CPAs for asymmetric catalysis

2 Combination of Mn with CPAs

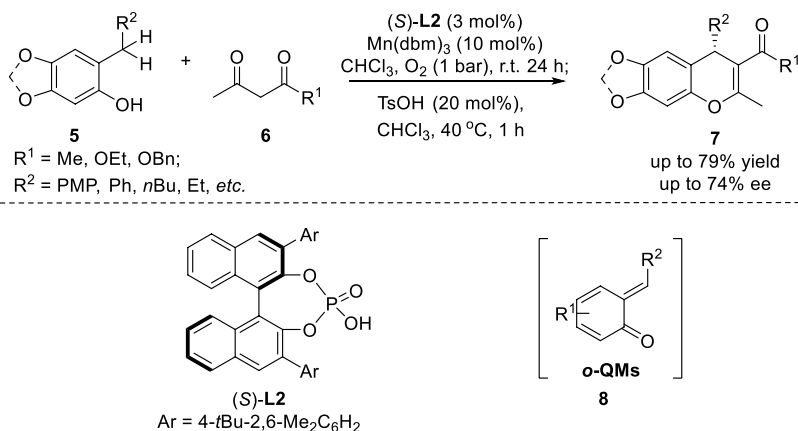
In 2010, List and co-workers developed a novel ion-pairing catalyst for the epoxidation of olefins **1** with PhIO **3** as a terminal oxidant [78]. As shown in Scheme 1, the ion-pairing catalyst contains an achiral Mn(III)–salen cation complex **4** and a chiral phosphate counteranion. Under optimized oxidative conditions, both acyclic and cyclic olefins react rapidly, furnishing the expected optically active oxiranes **2** in excellent yields and enantioselectivities (up to 96% ee). Remarkably, even styrenes bearing ether, nitro, ester, and cyano group were well applicable. This variant of Jacobsen–Katsuki epoxidation of alkenes [79] provides an efficient implementation of the concept of asymmetric counteranion-directed catalysis (ACDC) [29]. Mechanistically, the phosphate anion acts as a stereocontroller via communication with cationic intermediate, significantly stabilizing enantiomeric conformation of the cationic catalyst [e.g., Mn^{III}(salen) and the oxidation state O=Mn^V(salen)] [80].

Recently, Schneider and co-workers reported an asymmetric protocol for 4H-chromenes **7** synthesis via a relay manganese(III)/Brønsted acid catalysis (Scheme 2) [81]. The precatalyst Mn(dbm)₃ (Hdbm = dibenzoylmethane) provided a superior catalytic system for the conversion of 2-alkyl-substituted phenols **5** to ortho-quinone methide (*o*-QM, **8**) intermediates under an atmosphere of pure oxygen, followed by chiral BINOL phosphoric acid-promoted Michael addition with β-dicarbonyl compounds. The resulting chiral manganese monoposphate complex was identified as an effective catalyst in the addition process. Finally, products **7** were obtained via *para*-toluenesulfonic acid (TsOH)-promoted cyclodehydration sequence. The method was limited to the electron-rich phenols and the acyclic β-dicarbonyl compounds (including β-ketoesters and acetylacetone), and rigid β-dicarbonyls [82] were inapplicable because they could not act as a bidentate ligands.

Metal–organic frameworks (MOFs) have attracted increasing interest in recent years as a new family of porous crystalline hybrid materials as heterogeneous catalysts. In 2017, Liu and Cui [83] demonstrated that the chemical stability, catalytic activity, and enantioselectivity of chiral MOFs can be tuned simultaneously

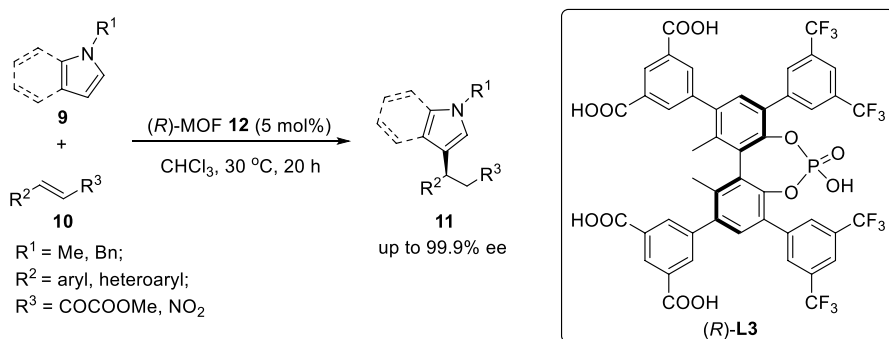


Scheme 1 Enantioselective epoxidation of olefins with Mn–salen phosphate complexes



Scheme 2 Asymmetric addition of β -dicarbonyls to ortho-quinone methides (*o*-QMs) via relay Mn(III) phosphate catalysis

by changing the steric and electronic effect of the ligand. Three porous chiral MOFs with the framework formula were prepared from different chiral CPA. As shown in Scheme 3, under both batch and flow reaction conditions, the CF_3 -containing MOF **12** from (*R*)-**L3** displayed excellent reactivity in the enantioselective alkylations of indoles and pyrroles **9** with electron-poor alkenes **10**. In contrast, the corresponding homogeneous catalysts gave targets **11** with low enantioselectivities.



Scheme 3 Enantioselectivity of metal–organic frameworks (MOFs) for alkylation of indoles and pyrroles

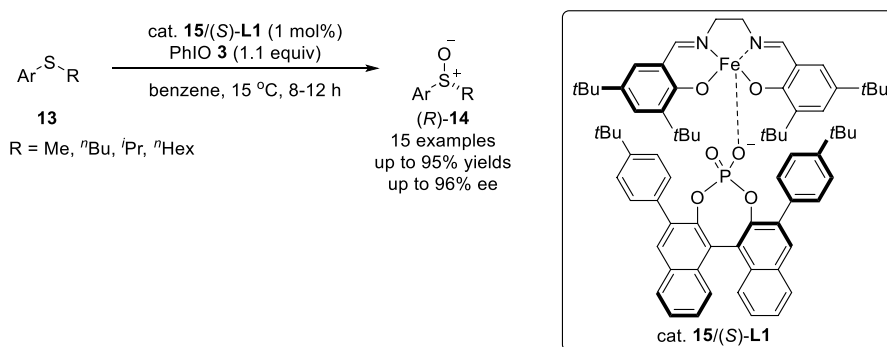
3 Combination of Fe with CPAs

3.1 Enantioselective Oxidations

Inspired by the study of ACDC chemistry [29] and the Mn(III)–salen system, in 2012, List and co-workers [84] reported an asymmetric oxidation of sulfides **13** with the combination of achiral Fe–salen cation **15** (Metallosalen) and chiral phosphate counteranion as an efficient oxygen-transfer catalyst (Scheme 4). The strategy utilized PhIO **3** as an oxidant and chiral iron–salen from (*S*)-**L1** as a catalyst. Thioethers **13**, especially the electron-poor and sterically bulky ones, underwent the oxidation reaction smoothly, resulting in chiral sulfoxides **14** with wide substrate scope, good yields and excellent enantioselectivities (up to 96% ee). This protocol disclosed the first application of asymmetric counteranion-directed catalysis to iron catalysis [52].

In 2016, Pappo, Toste and co-workers [85] designed a novel chiral iron(III)–BINOL phosphate complex Fe[(*R*)-**L1**]₃ as the catalyst for the enantioselective oxidative homo- and cross-couplings of 2-naphthols **16** and **16'**, allowing expedited access to 1,1'-bi-2-naphthols (*R*)-**17** with moderate-to-excellent yields and enantioselectivities (54–92% ee) (Scheme 5). The approach provided the first method for the synthesis of C₁- and C₂-symmetric BINOLs **17**, in which the 3- and 3'-positions are ready for further chemical transformations. Assisted by di-*t*-butyl peroxide (DTBP) **18** as an oxidant, a redox mechanism was proposed involving SET iron species, and a key radical-anion coupling step between the electrophilic naphthoxyl radical (**19**) and a second nucleophilic 2-naphthol(ate) partner (**16'**) to form species **20** (Scheme 5). Further oxidation and deprotonation provided product **17** efficiently with the aid of *t*BuO radicals.

In 2017, the Pappo group further used the resulting chiral iron phosphate generated from (*R*)-**L4** for asymmetric cross-dehydrogenative coupling reactions (Scheme 6) [86]. Current oxidation between 2-naphthols **16** and (–)-menthol-derived β-ketoesters **21** provided polycyclic hemiacetals **22** with good yields and diastereoselectivities (64–80% de). It is worth noting that the reaction temperature of 50 °C was crucial for inducing the combination of β-ketoesters **21**. Otherwise, a competitive oxidative radical-anion coupling with a second nucleophilic



Scheme 4 Enantioselective iron-salen-catalyzed sulfoxidation

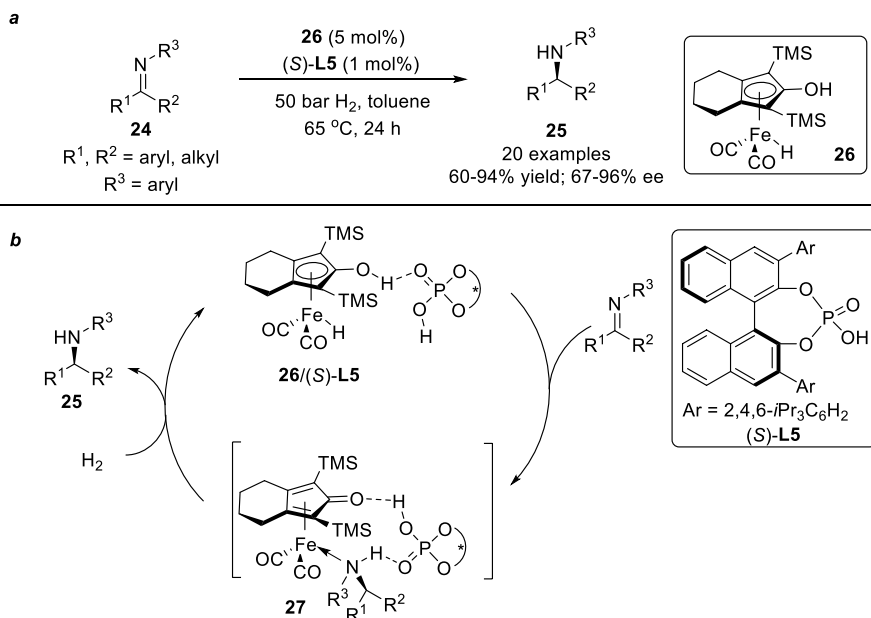
bounded naphthoxyl radical **23** followed by an intramolecular coupling afforded the expected polycyclic hemiacetal product **22**.

3.2 Enantioselective Reductions

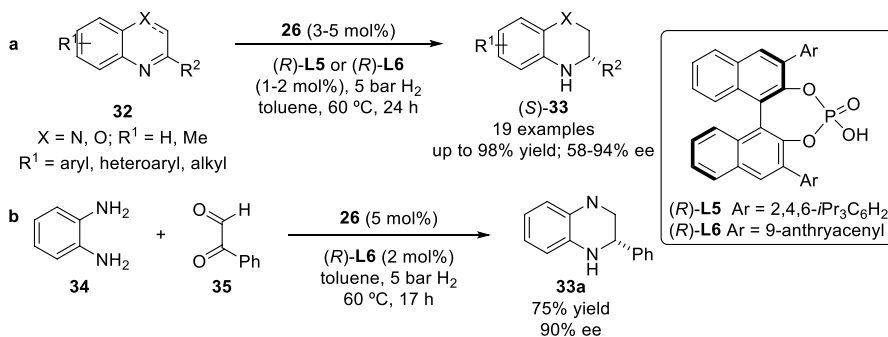
Recently, non-noble metal catalysts for the homogeneous hydrogenation of simple ketones and imines have been reported [87, 88]. The dual catalysis of achiral transition metal with chiral Brønsted acid offers an alternative route to promote asymmetric hydrogenation reactions [87, 88]. In 2011, Beller and co-workers [89] combined Knölker's iron complex **26** containing a cyclopentadienone ligand with a CPA, such as (*S*)-TRIP **L5**, to start an asymmetric hydrogenation of imine substrates **24** with molecular hydrogen as hydrogen donor (Scheme 7a) [90]. Based on the chiral anion-directed catalysis strategy, the expected amines **25** were obtained with 60–94% yields and excellent enantioselectivities (67–96% ee).

A general asymmetric hydrogen mechanism was proposed in Scheme 7b [90]. Knölker's iron complex **26** may coordinate with CPA (*S*)-**L5** to form a complex that possesses an iron hydride and an acidic hydrogen available for transfer to the polar imine moiety. The resulting reactive intermediate **27** is trapped by H₂ to regenerate the iron hydride **26**/(*S*)-**L5** complex and release **25**, thus accomplishing the asymmetric hydrogenation cycle.

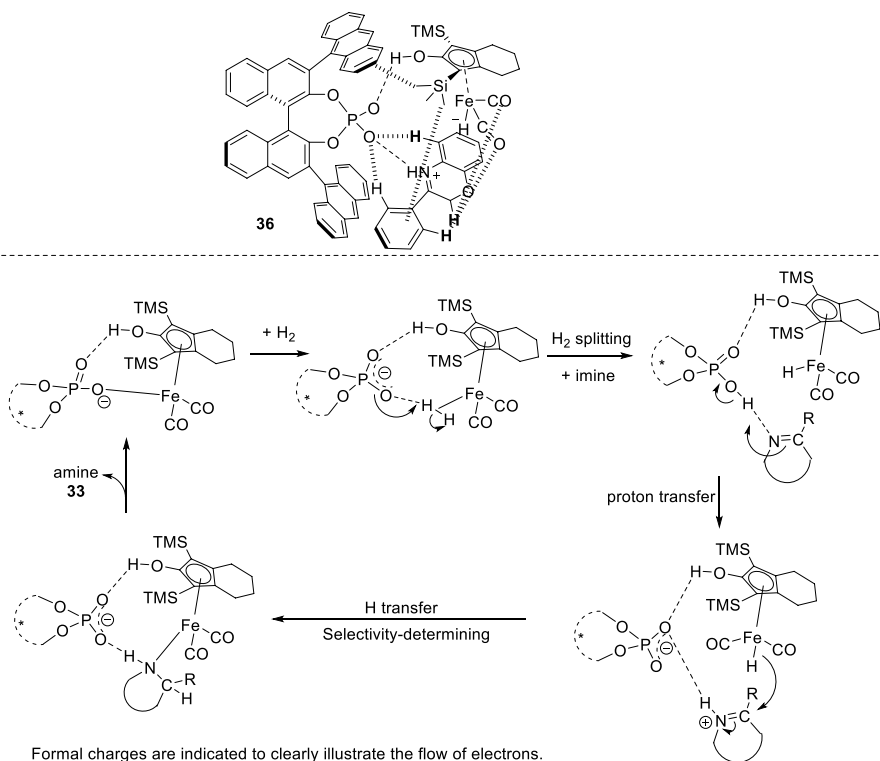
Taking into account the limitations in purification of the unstable ketimines **24**, the authors further developed the direct asymmetric reductive amination of ketones



Scheme 7 Cooperative iron and chiral phosphoric acid (CPA)-catalyzed asymmetric hydrogenation of imines



Scheme 10 Enantioselective hydrogenation of quinoxalines and 2*H*-1,4-benzoxazines



Scheme 11 Hopmann's mechanism of iron complex-catalyzed asymmetric hydrogenation

such cyclic imine benzoxazine substrates **32**, the reaction occurred with an involvement of noncovalent interactions (including electrostatic and dispersion interactions, as shown in **36**), that is, the hydroxycyclopentadienyl ligand and the iron complex do not change oxidation state during the catalytic cycle, rather than the redox mechanism. The H₂ splitting assisted by phosphate promotion is the rate-limiting step.

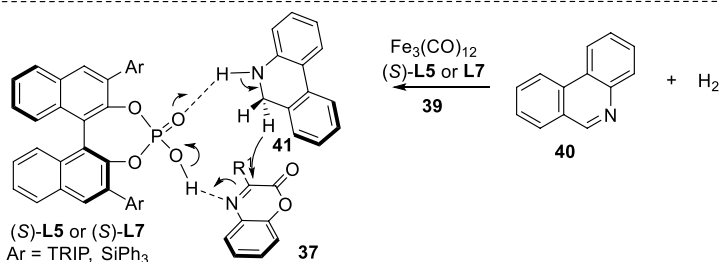
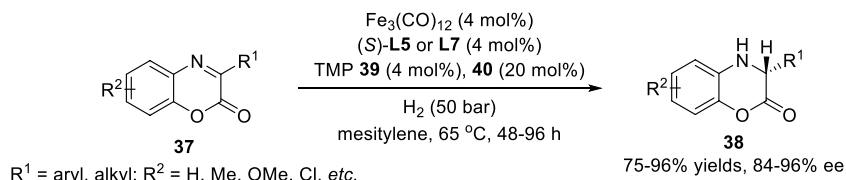
The subsequent stepwise hydrogenation of imine, where phosphoric acid acts as a proton donor, afforded the final product **33**.

In 2015, Beller's group reported an asymmetric hydrogenation of benzoxazinones **37** by a relay iron/chiral Brønsted acid catalysis (Scheme 12) [95]. Both chiral 3-aryl and, more challenging, 3-alkyl substituted dihydrobenzoxazinones **38** were obtained in good yields and uniformly high enantioselectivities (84–96% ee). Rather than the possible participation of chiral iron phosphate species, the authors proposed a relay catalytic mechanism involving $\text{Fe}_3(\text{CO})_{12}$ -catalyzed reduction of phenanthridine **40** to dihydrophenanthridine **41** in a molecular hydrogen atmosphere, and sequential asymmetric transfer hydrogenation of benzoxazinone **37**. The latter step, as depicted in Scheme 12, using a CPA catalyst (*S*)-**L7** provides a high level of enantioselectivity through a possible hydride transfer process. The achiral phosphine ligand tris(4-methoxyphenyl)phosphine (TMP) **39** effectively modulates the reactivity of $\text{Fe}_3(\text{CO})_{12}$ to decrease unselective background hydrogenations.

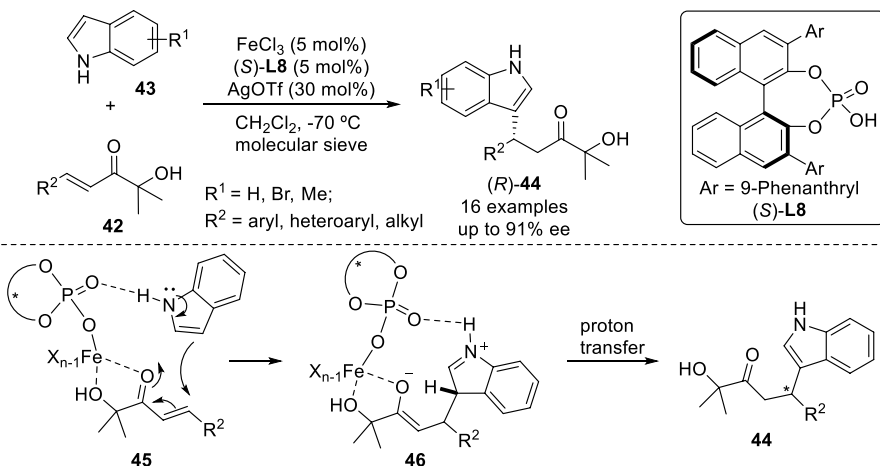
3.3 Enantioselective Additions

In 2009, Huang and co-workers reported an enantioselective Friedel–Crafts alkylation of indoles **43** with enones **42** by using iron(III) as Lewis acid and CPA as Brønsted acid to establish a binary catalyst (Scheme 13) [96]. Enones **42**, especially those having an electron-withdrawing group at the para position of the phenyl ring delivered chiral indoles (*R*)-**44** in good to excellent yields and enantioselectivities (up to 90% yield and 91% ee). In this catalytic system, the key catalytic species iron(III) phosphate salt (**45** and **46**) formed in situ was confirmed by electrospray ionization mass spectrometry (ESI–MS) studies, which seems to cause high activity and good enantioselectivity. The hydrogen-bonding interaction (**45** and **46**) between the basic site of CPA and indole **43** is important for the catalytic process.

Instead of proton transfer, an alternative protocol via selective β -proton elimination of the resulting carbocationic intermediate was developed by Luo and



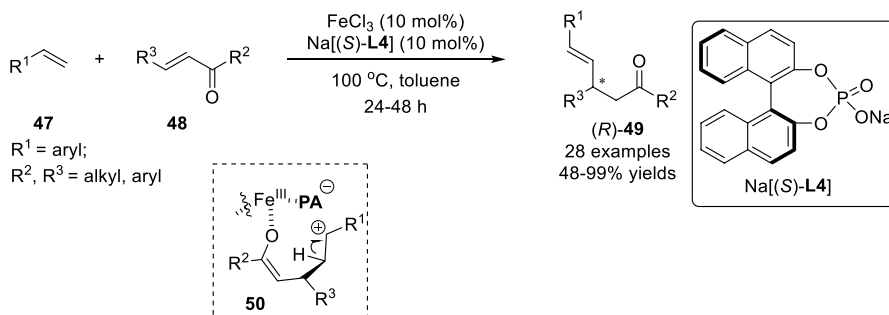
Scheme 12 Relay iron/chiral Brønsted acid-catalyzed hydrogenation of benzoxazinones **37**



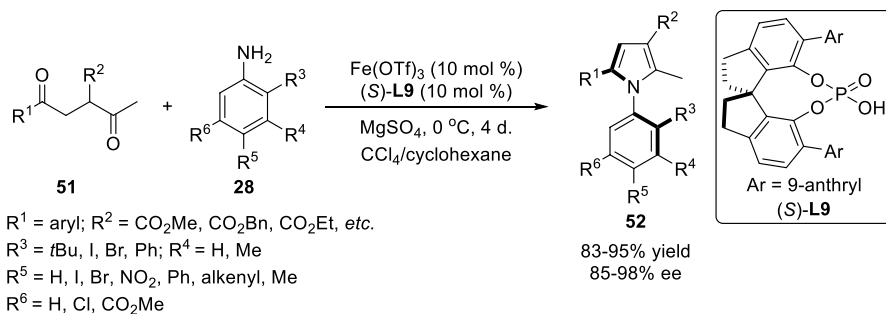
Scheme 13 Chiral iron(III) phosphate catalyzed Friedel–Crafts alkylation of indoles

co-workers in 2014 [97]. The authors combined FeCl_3 and sodium phosphate $\text{Na}[(S)\text{-L4}]$ to promote a direct conjugate nucleophilic addition of alkenes **47** to α,β -enones **48** (Scheme 14) [97]. A remarkably selective β -proton elimination of carbocationic intermediate **50** was revealed, wherein the anionic phosphate ligand was vital to inhibit cationic olefin polymerization and nucleophilic interception. The use of phosphate $(S)\text{-L4}$ provides better results than the corresponding acid. Further, an initial catalytic asymmetric version with the 3,3'-substituted phosphate ligand was conducted and gave 35% ee [97].

In 2017, Tan and colleagues developed the first asymmetric Paal–Knorr reaction under a simple binary iron/CPA catalysis (Scheme 15) [98]. 1,4-Diones **51** and substituted anilines **28** underwent the reaction smoothly in the presence of 10 mol% of $\text{Fe}(\text{OTf})_3$ and 10 mol% of $(S)\text{-L9}$ at 0 °C. This Paal–Knorr reaction allowed rapid access to a wide range of axially chiral arylpyrroles $(R)\text{-52}$ in good yields and enantioselectivities (85–98% ee). When using CCl_4/EtOH as co-solvent instead, $(S)\text{-52}$ was obtained.



Scheme 14 FeCl_3 -catalyzed direct conjugate addition of alkenes to α,β -enones

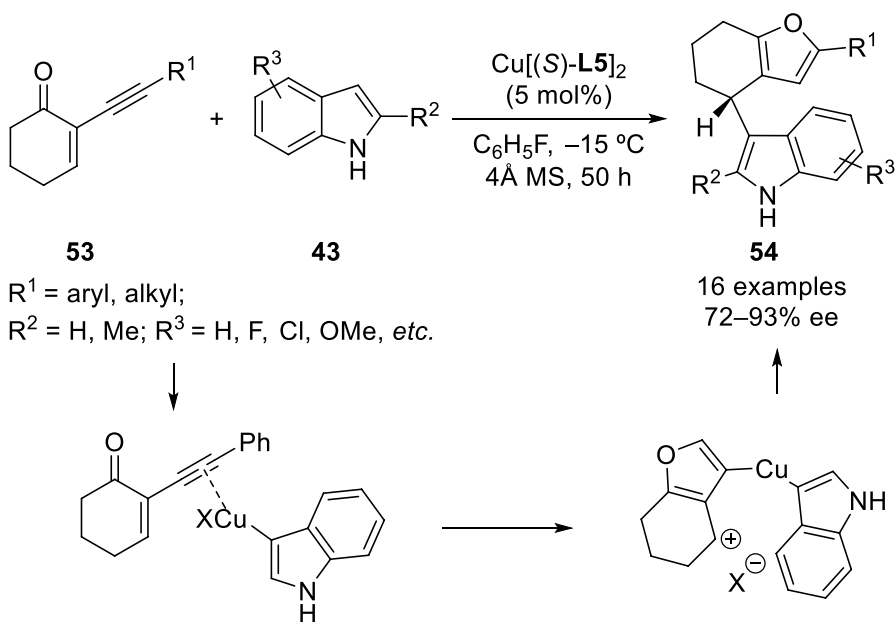


Scheme 15 Asymmetric iron-catalyzed Paal–Knorr reaction of 1,4-diones and anilines

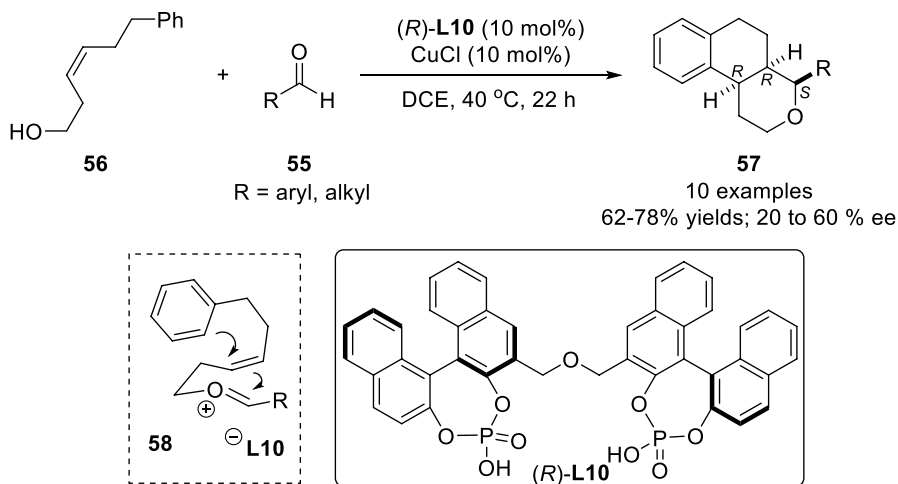
4 Combination of Cu with CPAs

4.1 Cyclizations

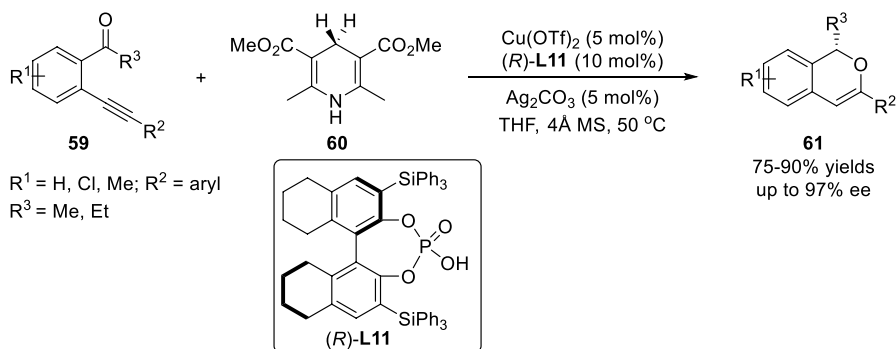
Cascade cycloisomerization reactions between carbonyl, imine, and alkenyl group or alkynyl group have provided a versatile tool for synthesis of heterocyclic scaffolds. In 2011, Toste's group developed a tandem cycloisomerization reaction for synthesis of furan derivatives **54** by using a chiral anionic copper(II) phosphonate catalyst (Scheme 16) [54]. Heterocyclization of 2-(1-alkynyl)-2-alkene-1-ones **53** followed by nucleophilic attack by indoles **43** yields products **54** with a high level of enantioselectivity (72–93% ee).



Scheme 16 Cu-catalyzed enantioselective cycloisomerization–indole addition reactions



Scheme 17 First enantioselective Prins cyclization



Scheme 18 Enantioselective synthesis of isochromene *o*-alkynylacetophenones

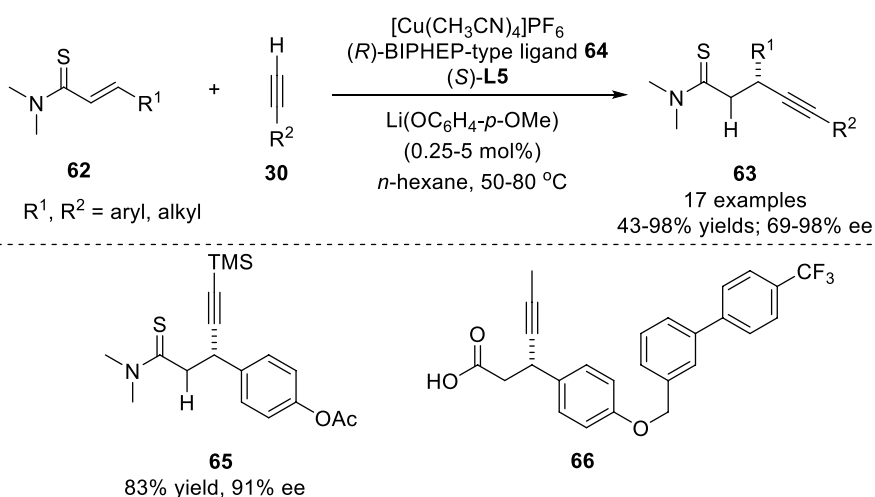
Lalli and van de Weghe developed the first catalytic enantioselective Prins cyclization in 2014 (Scheme 17) [99]. A superior binary-acid catalysis derived from CuCl and chiral BINOL-derived bis-phosphoric acid (*R*)-**L10** was used to activate the key oxonium ion intermediate **58** (through a hemiacetal pathway) and acted as a chiral counterion for enantioselective control [100, 101]. Treatment of aldehydes **55** and homoallylic alcohol **56** provides tetrahydropyrans **57** containing three contiguous stereogenic centers in high yields, good enantio- and excellent diastereoselectivities. The presence of a phenyl group as an internal nucleophile in homoallylic alcohol urges the tandem Prins/Friedel–Crafts process. The absolute configuration of **57** was confirmed as *4S,4aR,10bR* by single crystal X-ray analysis.

In addition to the sequential addition with nucleophiles, Akiyama and co-workers reported a chiral copper(II) phosphate-catalyzed enantioselective cycloisomerization/hydrogenation of *o*-alkynyl(oxo)benzenes **59** with Hantzsch esters **60** as a hydrogen source (Scheme 18) [102]. The reaction is believed to proceed

by sequential intramolecular cyclization and asymmetric transfer hydrogenation. This strategy furnishes an enantioselective synthesis of multisubstituted isochromenes **61** containing various substituents in high yields with good-to-excellent enantioselectivities.

4.2 Conjugate Additions

By using copper catalysis, Kumagai and Shibasaki described a direct catalytic asymmetric conjugate addition of alkynes to α , β -unsaturated thioamides in 2010 (Scheme 19) [103, 104]. The combined use of a soft copper(I) Lewis acid and a hard Brønsted base [e.g., Li(OC₆H₄-*p*-OMe)] resulted in simultaneous activation of alkynes **30** and thioamides **62**, giving the β -alkynylthioamide **63** with excellent enantioselectivity. The presence of (*S*)-**L5** enhances the basicity of Li(OC₆H₄-*p*-OMe), enabling promotion of reaction rate and enantiomeric control, especially for the success of aliphatic terminal alkyne **30**. While the (*R*)-**L5** was ineffective for the conversions, bisphosphine oxide was applied for aryl alkynes. Crystallography analysis showed Cu/(*R*)-**64**/(*S*)-**L5** association can be possible at the transition state. Based on the experiment results, the thioamide functional group was vital for the asymmetric alkynylation via coordination with copper alkynylide intermediates. Furthermore, the thioamide is readily converted into carboxylic acid, and thus the protocol has found useful synthetic application in a concise synthesis of a potent GPR40 agonist AMG 837 **66** via the formation of chiral alkyne intermediate **65** [105].

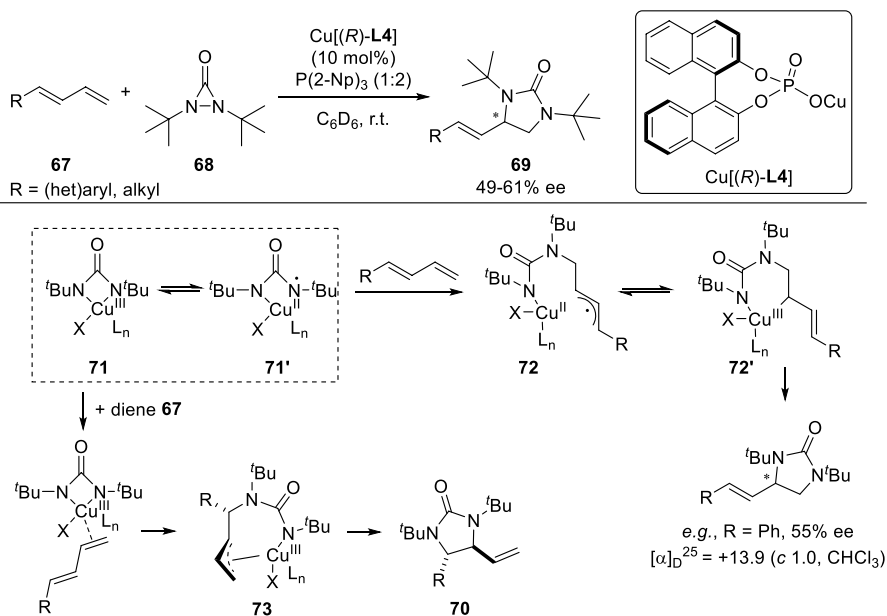


Scheme 19 Asymmetric conjugate addition of terminal alkynes to α , β -unsaturated thioamides

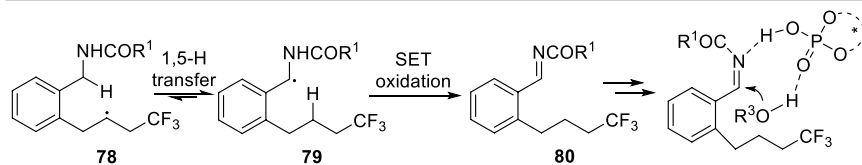
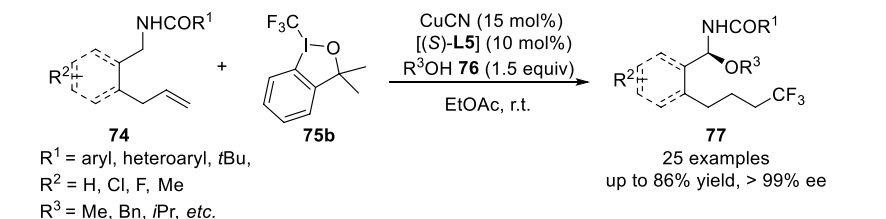
4.3 Radical-Involved Transformations

Recently, Shi and co-workers established a simple protocol for assembling vicinal diamines from conjugated dienes **67** with 1,3-*di-tert*-butyldiaziridinone **68** as nitrogen source [106]. The copper salt CuX-PPh₃ (1:2) was applied to the diamination reaction, and provided the diaminated products **69** in excellent yields and terminal regioselectivities (Scheme 20) [107]. It was found that the chiral copper(I) diphenyl phosphate produced from mesitylcopper(I) and the corresponding phosphoric acid (*R*)-**L4** achieve an asymmetric diamination process in moderate enantiomeric excesses (49–61% ee), where the catalyst provides an anionic counterion effect. As illustrated in Scheme 20, two distinct mechanistic pathways for Cu(I)-catalyzed diamination were proposed to account for the different regioselectivity at either the terminal or internal double bond affected by the reaction conditions. First, in the presence of copper(I) catalyst Cu[(*R*)-**L4**], the N–N bond of **68** is activated and forms a Cu(II) nitrogen radical **71'** or a four-membered Cu(III) species **71**. The Cu(II) nitrogen radical **71'** further reacts with the conjugated diene **67** to form a new Cu(II) allyl radical species **72** or a Cu(III) complex **72'**, which ultimately results in the terminal diaminated product. While under simple CuBr catalysis, the four-membered Cu(III) species **71** reacts with dienes **67**, providing the internal diamination target **70** through π -allyl species **73** [108, 109].

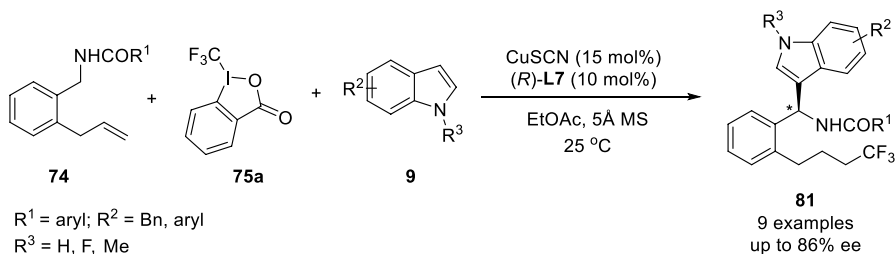
In contrast to the well-documented enantioselective nucleophilic and electrophilic transformations, asymmetric radical chemistry still remains a formidable challenge owing to the high reactivity of such free radical species [71, 72, 110–112]. To address this problem, Liu and co-workers developed a dual-catalytic method that



Scheme 20 Diamination of conjugated dienes with 1,3-*di-tert*-butyldiaziridinone



Scheme 21 Enantioselective remote C–H bond functionalization of unactivated alkenes



Scheme 22 Enantioselective α -C–H functionalization of amides with indoles

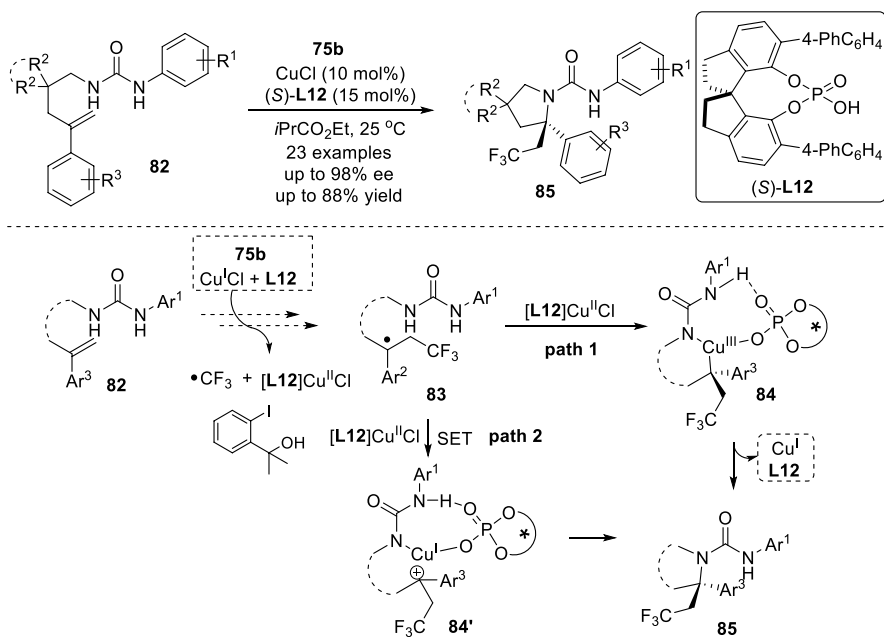
combines copper and CPA to handle these intrinsically reactive species and further capture different nucleophiles to create new bonds [113]. In 2014, they reported the first example of highly enantioselective radical trifluoromethylation of alkenes which uses a dual copper(I)/CPA catalytic system for simultaneous installation of two new C–CF₃ and C–O bonds (Scheme 21) [53]. This multicomponent protocol produces a wide range of valuable enantioenriched trifluoromethylated *N,O*-aminals **77** with good to excellent yields and with excellent regio-, chemo-, and enantioselectivities. The reaction is initiated by addition of the in situ generated trifluoromethyl radical to unactivated alkenes **74** to generate **78** under Cu(I)/CPA catalysis with Togni's reagent **75b**, followed by a 1,5-hydrogen atom transfer to give a new C-centered radical **79** adjacent to nitrogen atoms. A further single-electron oxidation step produces the imine intermediate **80**. The attack of an alcohol to imine through a two-point hydrogen bonding interaction in the presence of CPA via a zwitterionic transition state yields the final product. Functionalized primary and secondary alkyl and benzyl alcohols **76** were applicable for the reaction.

Similar to the enantioselective attack of alcohols with *N*-(2-allylbenzyl)amides **74**, the use of *N*-benzyl or aryl substituted indoles **9** instead of alcohols as a nucleophile efficiently leads to two new C–CF₃ and C–C(sp²) bonds in a one-pot manner (Scheme 22) [114]. Under the synergistic catalytic system of CuSCN and (*R*)-L7, the reaction provides a simple and straightforward method to access various

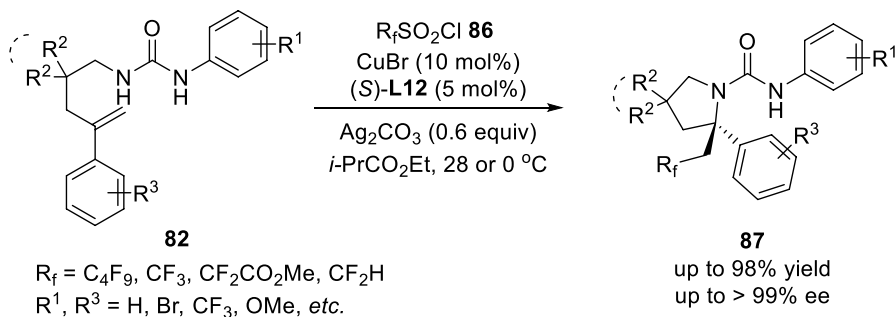
trifluoromethylated indole compounds **81** in moderate to good yields and enantioselectivities (up to 86% ee).

In 2016, Liu and co-workers disclosed a novel asymmetric radical aminotrifluoromethylation of alkenes **82** for the first time, providing straightforward access to densely functionalized CF₃-containing pyrrolidines **85** bearing an α -tertiary stereocenter with excellent enantioselectivity (Scheme 23) [115]. The key to success is not only the utilization of a Cu(I)/CPA dual-catalytic system but also the use of urea (**82**) bearing two acidic N–H as both the nucleophile and directing group. The in situ generated trifluoromethyl radical from **75b** would attack the alkene to provide a benzylic radical intermediate **83**. The benzylic radical and urea could be trapped by Cu(II) phosphate to generate a Cu(III) species **84** (path 1) followed by reductive elimination to forge the C–N bond formation. An alternative SET process between benzylic radical and Cu(II) phosphate to yield the carbocation intermediate **84'** and subsequent C–N bond formation is also possible (path 2). The stereoselectivity of this process was probably controlled by chiral phosphate (*S*)-**L12** via both hydrogen-bonding interactions with N–H bond adjacent to aryl group and ion-pairing interaction in a concerted transition state.

Besides the radical trifluoromethylation with Togni's reagent, commercially available fluoroalkylsulfonyl chlorides **86**, such as CF₃SO₂Cl, *n*-C₄F₉SO₂Cl, CH₃O₂CCF₂SO₂Cl, etc. were also suitable as precursors for aminoperfluoroalkylation and aminodifluoromethylation of alkenes **82** (Scheme 24) [116]. The method provides a sustainable, widely applicable and remarkable enantioselective platform for efficiently obtaining four types of enantioenriched functionalized α -tertiary



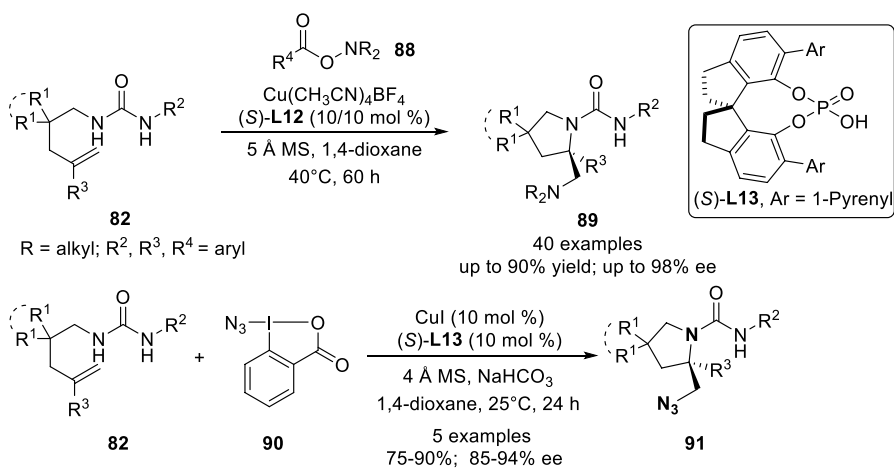
Scheme 23 Asymmetric radical aminotrifluoromethylation of alkenes



Scheme 24 Asymmetric radical aminoperfluoroalkylation and aminodifluoromethylation of alkenes

pyrrolidines **87** bearing different β -fluoroalkyl groups. It is worth noting that the use of silver carbonate can absorb in situ generated HCl and inhibit background and side hydroamination reactions.

Based on the cooperative Cu(I)/CPA catalysis, Liu's group further extended the strategy to diamination and azidoamination of unactivated alkenes by using *O*-acylhydroxylamines **88** and azidoiodinane **90** as *N*-radical precursors, respectively [117]. As shown in Scheme 25, these transformations enable a facile and selective route to enantioenriched α -tertiary pyrrolidines **89** bearing a β -alkylamine and azido moiety with good yields, giving two C–N bonds in one-pot manner. The results indicated that urea **82** bearing electron-withdrawing *N*-aryl group is key to the success of conversions. The current program provides a complementary and efficient method for the synthesis of various chiral vicinal diamines **89** and **91**, such as β -primary, secondary, or tertiary amine-containing pyrrolidines, and bicyclic amines. Further, an asymmetric copper-catalyzed aminoarylation of urea-derived alkenes was also established, and provided the

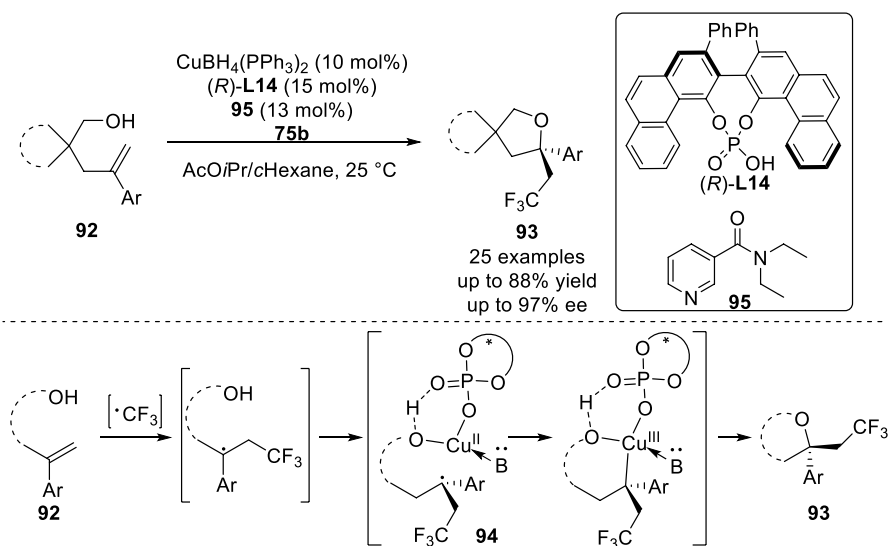


Scheme 25 Copper-catalyzed asymmetric radical diamination of alkenes

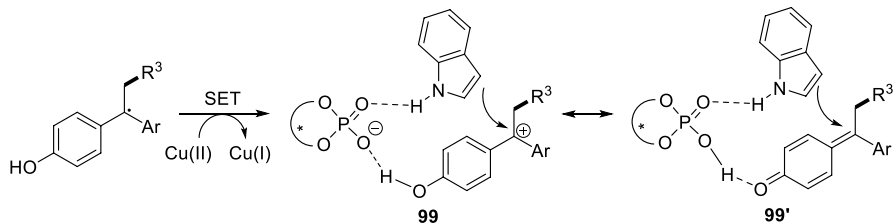
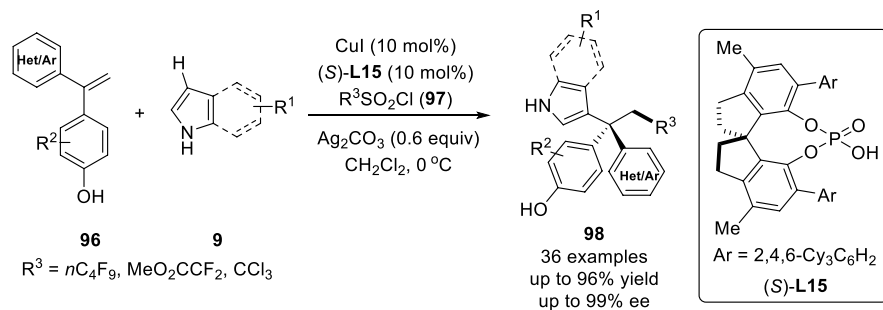
expected chiral pyrrolidines with good yields and enantioselectivities [118]. Aryldiazonium salts with methylsulfonyl and nitro group at phenyl moiety were used as the aryl radical precursor. Very recently, a variant of enantioselective radical aminosilylation with alkene **82** with $(\text{TMS})_3\text{SiH}$ was developed by Liu's group using Cu(I)/CPA cooperative catalysis [119].

Liu's group revealed that alcohols are also appropriate for asymmetric radical reactions. They treated alkenes **92** with a pendant intramolecular alcohol moiety with **75b** under copper(I)/phosphoric acid and realized asymmetric oxytrifluoromethylation (Scheme 26) [120]. Conversion with cooperative $\text{CuBH}_4(\text{PPh}_3)_2$ /chiral VAPOL-based acid catalysis (*R*)-**L14** provides various trifluoromethyl-substituted tetrahydrofurans **93** bearing an α -tertiary stereocenter with excellent enantioselectivity. Remarkably, the presence of achiral pyridine (e.g., *N,N*-diethylnicotinamide **95**) was vital to the radical oxytrifluoromethylation to improve the enantiotopic selectivity, which was considered as a coordinative ligand on copper metal (**94**) to stabilize the high-valent copper species in the asymmetric control process.

Very recently, the authors completed the asymmetric intermolecular dicarbofunctionalization of 1,1-diarylalkenes **96** catalyzed by a dual Cu(I) and sterically bulky SPINOL phosphoric acid (*S*)-**L15** with diverse carbon-centered radical precursors **97** and electron-rich heteroaromatics **9** (Scheme 27) [121]. This three-component radical reaction provides direct access to chiral triarylmethanes **98** bearing quaternary all-carbon stereocenters with high efficiency as well as excellent chemo- and enantioselectivities. Various sulfonyl chlorides **97** and Togni's reagent were applied to C-centered radicals. DFT calculations elucidated that hydrogen-bonding and ion-pair interactions between CPA and substrates (N-H and O-H moieties, as shown in **99** and resonance **99'**) creates a chiral environment



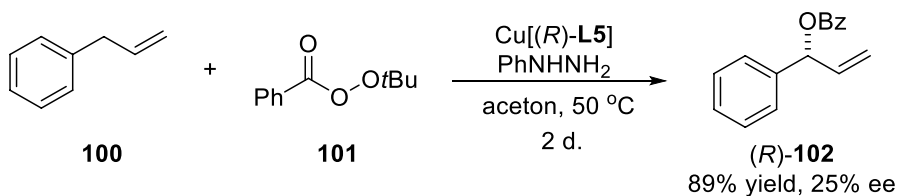
Scheme 26 Asymmetric radical oxytrifluoromethylation of alkenes with alcohols



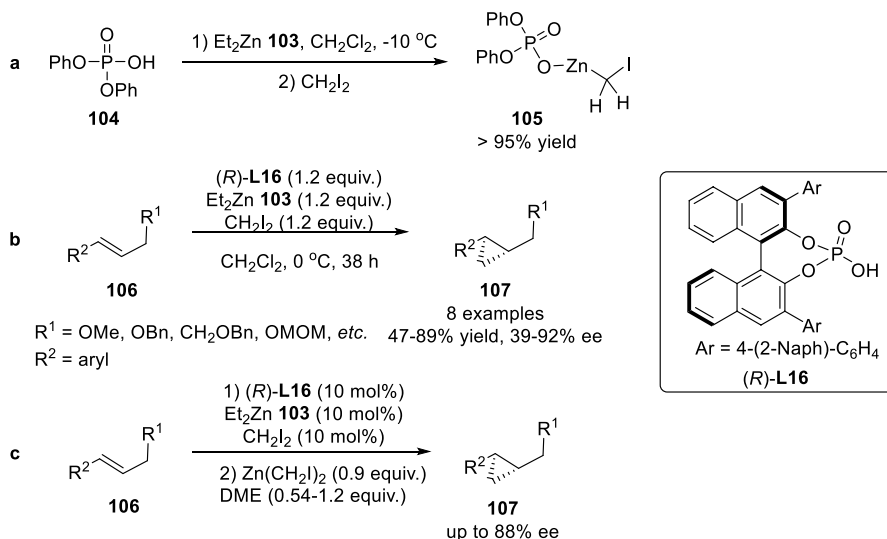
Scheme 27 Asymmetric radical 1,2-dicarbofunctionalization of alkenes with heterocycles

for enantiodiscrimination. The incorporation of a hydroxy group as the directing group, and introduction of a sterically demanding CPA will favor the desired radical difunctionalization over the otherwise remarkable side reactions.

The effect of chiral copper(I) phosphates generated from BINOL-derived phosphoric acids on Kharasch–Sosnovsky of acyclic alkenes **100** were evaluated in 2015 (Scheme 28) [122]. It is proposed that peroxybenzoate **101** converts Cu(I) to copper(II) benzoate and *O**t*Bu radical. The latter abstracts the allylic hydrogen atom to product a key allylic radical species. The combination of copper(II) benzoate and allylic radical species provides the allyl ester **102** in good regioselectivity but low enantioselectivity.



Scheme 28 Cu-catalyzed asymmetric allylic oxidation of linear alkenes



Scheme 29 Cyclopropanation of alkenes with iodomethylzinc phosphates

5 Combination of Zn with CPA

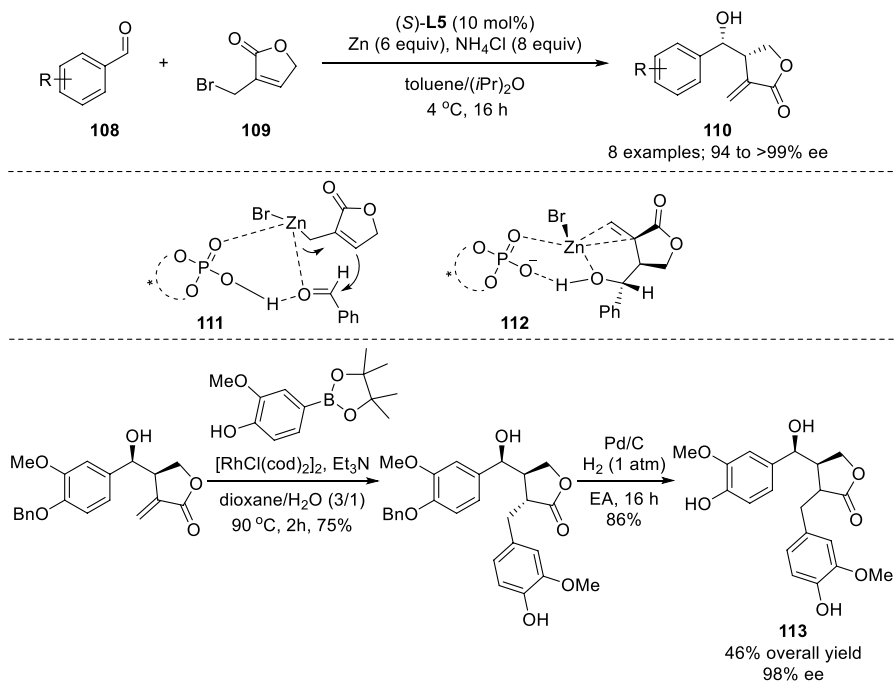
Charette and colleagues [123–125] first introduced iodine methyl zinc phosphate **105** as a new available cyclopropanation reagent in 2005, providing a method for asymmetrical Simmons–Smith cyclopropanation of alkenes (Scheme 29). A strong background reaction without the phosphate catalyst always occurs, which prevents high enantiopurity. Initial attempts at the racemic reaction were conducted with diphenylphosphate **104** and diethylzinc **103** (Scheme 29a). The results showed that **105** was obtained in excellent yield, and was quite stable and crystallized as a dimeric structure possessing tetrahedral geometry with respect to the Zn atom (Scheme 29a). Afterwards, the iodomethylzinc phosphate **105** was extended for the cyclopropanation reaction with alkenes and the reaction furnished the expected products in good yields. Upon treatment of the reaction with chiral zinc phosphate derived from (*R*)-**L16** with cinnamyl alcohol and homoallylic ether **106**, the desired cyclopropanes **107** were obtained in very good yields and excellent enantioselectivities. Different additives were optimized to prevent the use of a stoichiometric amount of phosphoric acid (*R*)-**L16** (1.2 equivalents). They finally identified that the addition of 0.5 equivalent of dimethyl ether (DME) and 0.9 equivalent of $\text{Zn}(\text{CH}_2\text{I})_2$ could reduce the (*R*)-**L16** to catalytic amount with a slight loss of enantioselectivity (up to 88% ee, Scheme 29c).

Analogously, Charette's group applied the chiral zinc TADDOL phosphate species to the cyclopropanation of allylic ethers and 1-phenyl-3,4-dihydronaphthylene [126]. Allylic ethers showed more reactivity than unfunctionalized olefins, resulting in high yields and selectivity (up to 75% ee). They also identified (*n*-BuO)₂P(O)OZnCH₂I derived from dibutyl phosphate as a very stable reagent and extended this to the cyclopropanation reactions [127]. The substrate scope was very broad,

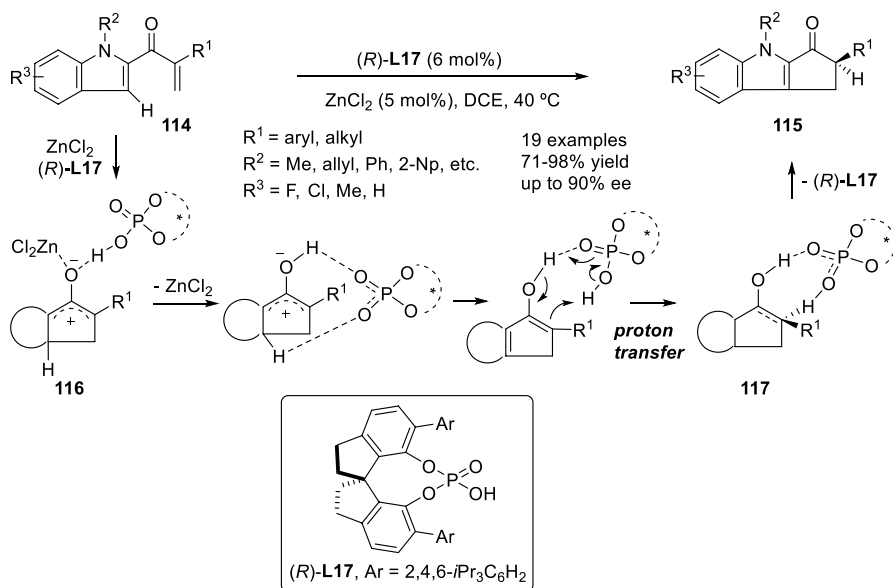
including allylic alcohols and their derivatives, styrenic substrates with electron-donating or electron-withdrawing substituents on the aromatic ring, and even unfunctionalized alkenes were applicable to afford the desired cyclopropanes in excellent yields (72–99%).

Recently, Orthaber and Faber [128] developed an asymmetric allylation of (hetero)aromatic aldehydes **108** with the in situ generated zinc(II)-allylbutyrolactone species from **109** (Scheme 30). Catalyzed by CPA (*S*)-**L5**, the Barbier-type allylation results in β -substituted α -methylenebutyrolactones **110** in good yields and enantioselectivities. NH_4Cl is a key additive to activate Zn surface. Based on the experimental observations and DFT studies, the proton of CPA has an important influence on the success of allylation of activated aldehydes **108**, and chiral induction occurs by forming key zinc complexes (**111** and **112**) bearing a six-membered ring in the transition state, as shown in Scheme 30. Unfortunately, aliphatic aldehydes provided the products only in low enantioselectivities. This allylation strategy has witnessed synthetic applications, such as in the concise synthesis of natural product (*S*)-(-)-hydroxymatairesinol **113** in 46% overall yield and 98% ee.

Enantioselective control of tertiary α -carbon in the Nazarov cyclization of enones is challenging because the reaction involves an enantioselective proton transfer process. In 2017, Zhou and Zhu [129] developed a scalable, highly enantioselective Nazarov cyclization of indole enone substrates **114** bearing one coordinating site. The reaction was cooperatively catalyzed Lewis acid (ZnCl_2) and a chiral Brønsted acid (*R*)-**L17** (Scheme 31). The mechanism studies by DFT calculation and



Scheme 30 Asymmetric allylation reaction for synthesis of α -methylenebutyrolactones



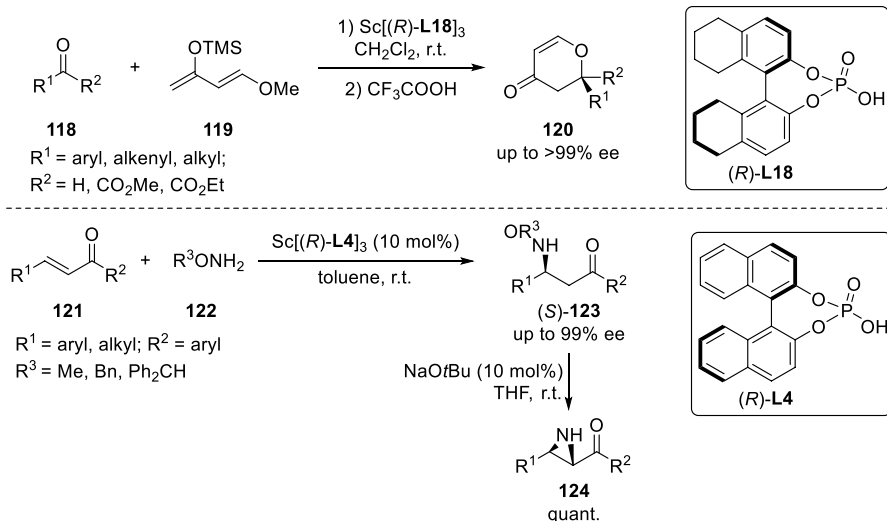
Scheme 31 Enantioselective zinc(II)-catalyzed Nazarov cyclization of indole enones

experimental results showed that both $(R)\text{-L17}$ and Zn(II) ionic activate the enone by coordination to promote cyclization and produce carbocation species **116**. Then, ZnCl_2 dissociation and CPA-catalyzed [1,3]-proton transfer through the eight-membered transition state **117** to selectively provide a Nazarov cyclized target **115**. The proton transfer of the enol intermediate is the stereochemistry-determining step of the process.

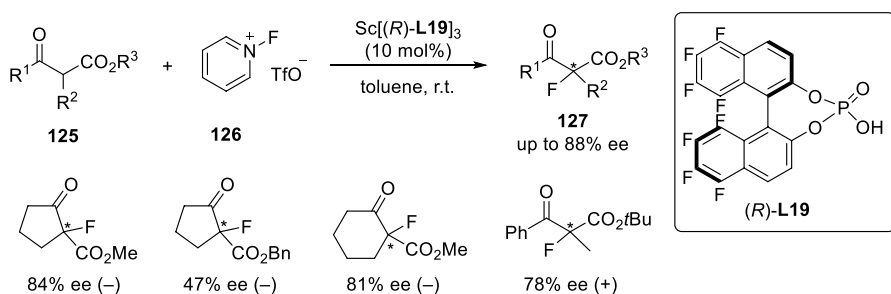
6 Combination of Sc with CPA

As early as in 1998, Inanaga and co-workers [130] first reported chiral rare-earth-metal phosphate catalysts in the enantioselective hetero-Diels–Alder reaction. In this platform, scandium organophosphate complexes, $\text{Sc}[(R)\text{-L4}]_3$, $\text{Sc}[(R)\text{-L18}]_3$ could act as homogeneous Lewis acid catalysts for the enantioselective hetero-Diels–Alder reactions [131, 132]. As shown in Scheme 32, treating carbonyl compounds **118** with Danishefsky's diene **119** afforded the corresponding cycloadducts **120** with excellent ee values.

Inanaga et al. [133–135] further introduced chiral scandium complex $\text{Sc}[(R)\text{-L4}]_3$ into the aziridination of chalcone **121** with *O*-substituted hydroxylamines **122** to provide optically active α -keto aziridines **124** with good enantioselectivity (Scheme 32). The reaction occurred by an enantioselective Michael addition to generate **123**, followed by treatment with $\text{La}(\text{O}i\text{Pr})_3$ or sodium *tert*-butoxide to give the target aziridine-ring (αR , βS)-**124** in quantitative yields and without loss of ee values.



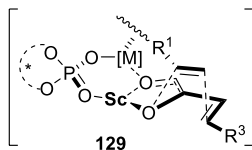
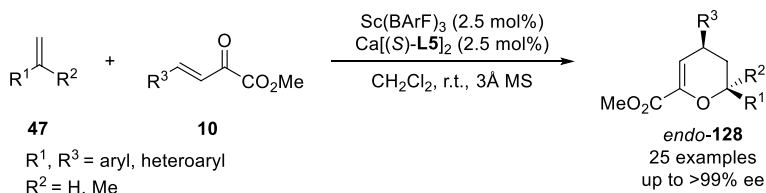
Scheme 32 Scandium phosphate-catalyzed hetero-Diels–Alder reaction and conjugate addition



Scheme 33 Asymmetric fluorination of β -keto esters with 1-fluoropyridinium triflate

In 2006, Inanaga's group identified the perfluorinated phosphate complex $\text{Sc}[(R)\text{-L19}]_3$ as a chiral catalyst in the fluorination reaction of β -ketoesters **125** with electrophilic 1-fluoropyridinium triflate **126** (Scheme 33) [136]. The presence of fluorine atom in $\text{Sc}[(R)\text{-L19}]_3$ is critical and causes a stronger Lewis acidity than its analogous $\text{Sc}[(R)\text{-L4}]_3$. Under simple conditions, both cyclic and acyclic dicarbonyl substrates **125** were applicable for the asymmetric fluorination to provide **127** with high enantioselectivities (up to 88% ee).

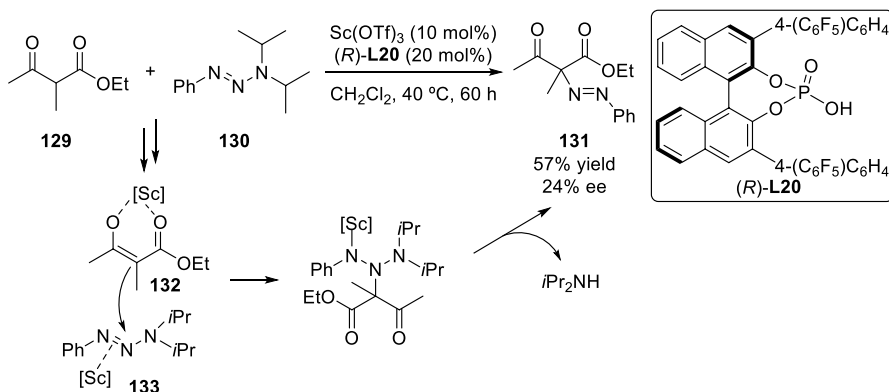
In 2013, Luo and co-workers [61] published a highly selective [4+2] cycloaddition of olefins **47** with β , γ -unsaturated α -ketoesters **10** (Scheme 34). Significant binary catalysis with $\text{Sc}(\text{BARF})_3$ [$\text{BARF} = [3,5\text{-}(\text{CF}_3)_2\text{C}_6\text{H}_3]_4\text{B}$] and chiral calcium phosphate proved to be effective for the synthesis of endo-cycloaddition products **128** in excellent diastereoselectivity (Scheme 34). Based on the literature and experimental observations, a bidentate activation (**129**) between ketoester **10** and



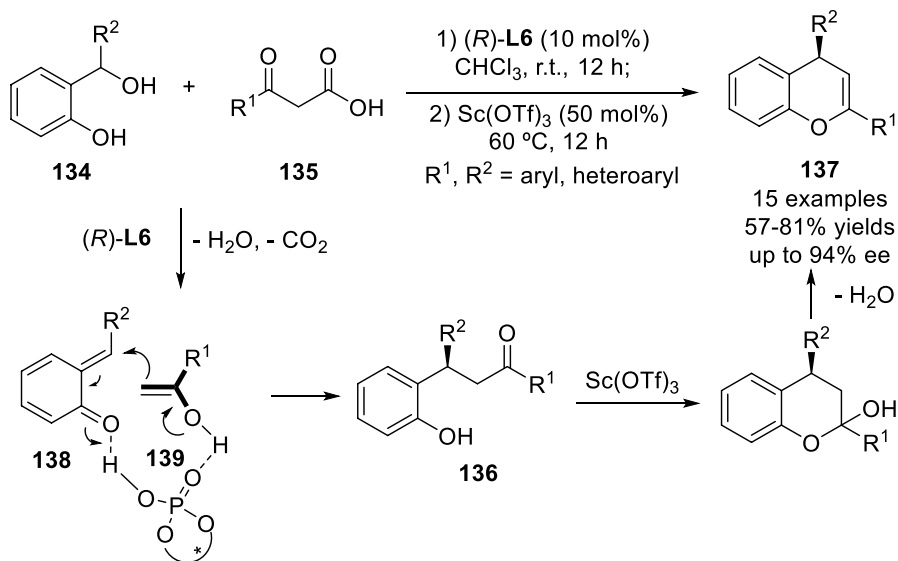
Scheme 34 Asymmetric binary acid-catalyzed [4+2] cycloadditions with simple olefins

the cationic scandium metal center was proposed to promote the reaction. The TRIP group of ligands (*S*)-**L5** in complex with Ca/Sc constitute a well-defined chiral environment that tunes the orbital-favored and less-space-demanding endo transition state (Scheme 34).

In 2014, Luo and co-workers developed a new intermolecular azo-transfer of aryl triazenes **132** with 1,3-dicarbonyl compounds under $\text{Sc}(\text{OTf})_3$ catalysis (Scheme 35) [137]. The combination of Sc(III)-activated triazenes **133** and enol ether species **132** completed a conjugate addition and a N–N bond cleavage providing aliphatic azo compounds **131** with good yields and wide substrate scopes. However, an initial catalytic asymmetric variant with (*R*)-**L20** showed a disappointing ee value (24% ee).



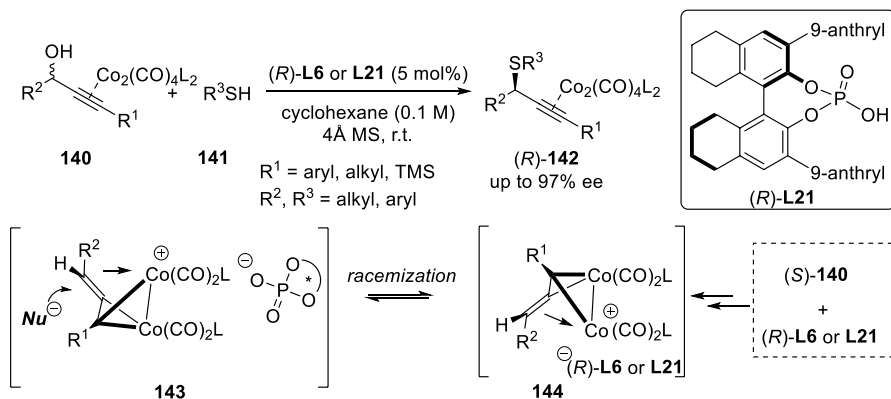
Scheme 35 $\text{Sc}(\text{OTf})_3$ -catalyzed transfer diazenylation of dicarbonyl compounds with triazenes



Scheme 36 Enantioselective decarboxylative alkylation of β -keto acids to form chiral benzopyrans

7 Miscellaneous

Very recently, Kim and co-worker [138] developed a gram-scale asymmetric synthesis of 2,4-diaryl-1-benzopyrans **137** via a one-pot two-step transformation (Scheme 36). With the aid of (*R*)-**L6**, the β -keto acid **135** is efficiently subjected to a decarboxylative process to provide an enol intermediate **139** at room temperature, which then reacts with ortho-quinone methide **138** in situ generated from *o*-hydroxy benzylic alcohol **134** to produce the chiral adduct **136**. Subsequently, $\text{Sc}(\text{OTf})_3$ promotes the cyclization and dehydration sequence to give synthetically



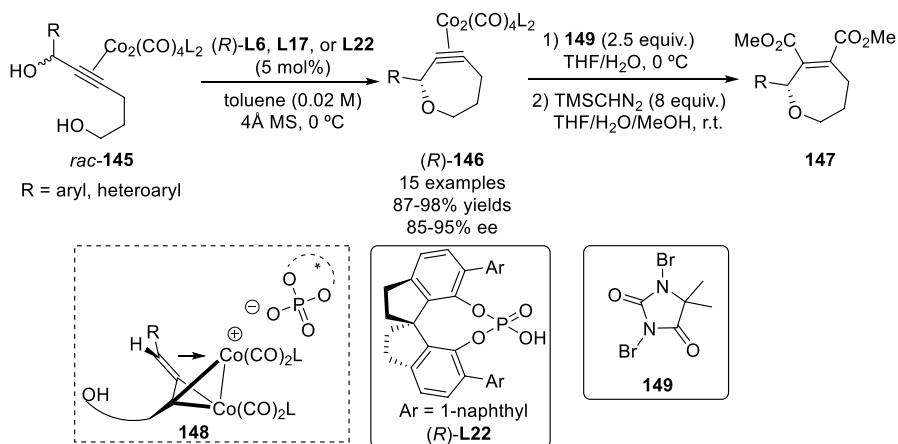
Scheme 37 Nucleophilic substitution reaction of racemic alkyne-dicobalt complexes with thiols

useful chiral benzopyrans **137** in good yields and enantioselectivities (up to 94% ee).

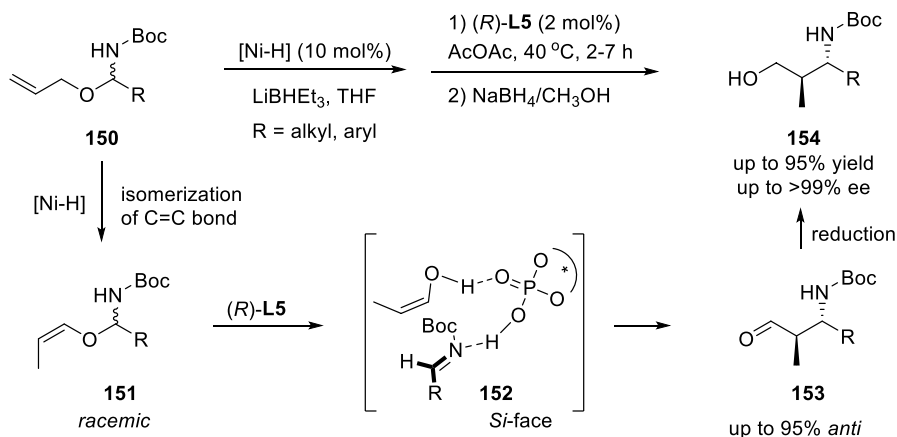
Compared to the enantioselective nucleophilic substitution reactions at the prochiral sp^2 -hybridized carbon atom, the involvement of sp^3 -hybridized carbon atom has been underdeveloped [139]. In 2016, Terada and co-workers developed a novel nucleophilic addition of thiols **141** to the racemic alkyne–dicobalt complex **140** derived from the corresponding secondary propargylic alcohols (Scheme 37) [140]. A key planar cobalt-based carbenium ion **143** was probably formed by phosphoric acid-catalyzed rearrangement and stabilized by the conjugate base phosphate anion (*R*)-**L6** or **L21**. The racemization process is markedly quick over nucleophilic addition with thiols **141**, enabling better results for addition conversion. Increasing temperature would advance the enantioconvergent of (*S*)-substrate **140** to intermediate **144** for forming (*R*)-configured product **142**.

Further, the authors developed an intramolecular enantioconvergent Nicholas reaction version to synthesize seven-membered cyclic ethers **147** in high yields with good enantioselectivities (Scheme 38) [141]. In the presence of CPAs, racemic diols **145** containing an (hetero)aryl substituent at the propargylic position reacted efficiently via key intermediates **148**. The resulting enantioenriched cyclic ethers (*R*)-**146** were further treated in one-pot manner with 1,3-dibromo-5,5-dimethylhydantoin **149** for de-complexation, to afford densely functionalized cyclic ethers **147** bearing an unsaturated diester moiety without loss of enantiomeric excess.

In 2009, Terada's group reported a highly enantioselective synthesis of optically active anti β -amino alcohols **154** (Scheme 39) [142, 143]. Under optimal conditions, various racemic hemiaminal allyl ethers **150** bearing alkyl-, benzyl- and phenyl-substituents at the β -position were well applicable. A Ni(II) complex catalyzed the olefin isomerization of starting material **150** to racemic hemiaminal vinyl ethers **151**, followed by a CPA catalyzed aza-Petasis–Ferrier reaction (e.g., (*R*)-**L5**) to afford the β -amino aldehydes **153** via key intermediate **152**. The racemic vinyl ethers **151** underwent a sequential C–O bond cleavage and C–C bond



Scheme 38 Enantioselective intramolecular Nicholas reaction of racemic diols



Scheme 39 Alkene isomerization/enantioselective aza-Petasis–Ferrier rearrangement reaction of hemiaminal vinyl ethers

formation to form β -amino aldehydes **153** with high level of anti-, diastereo- and enantioselectivities (up to 99% ee). Finally, a formyl reduction by NaBH_4 /methyl alcohol yielded the β -amino alcohol compounds **154**.

8 Conclusions and Prospects

In this chapter, we have provided an overview of the development and applications of organic phosphoric acids in combination with different first-row transition metals in asymmetric catalysis, providing a mechanistic discussion to better understand the interaction of the metal/phosphate and the factors for asymmetric control. The combination of metal cations/complexes with phosphates provides a variety of catalytic modes, including relay catalysis, counterion-pairing catalysis, and binary-acid catalysis, thus enabling a range of enantioselective transformations. This progress represents an essential part of the implement of asymmetric counteranion-directed catalysis reported so far. In addition, concerning the property of metals, e.g., copper, iron, and manganese can act as one or two-electron transfer catalysts to permit redox reactions. Significant efforts in enantioselective oxidations and hydrogenations, C–H bond functionalizations and radical-initiated difunctionalizations of olefins have been made recently. Consequently, the complexity and diversity of the catalytic systems between first-row transition metals and phosphate derivatives potentially provide a powerful, viable and accessible route for asymmetric synthesis, although it is still less developed and limited to some transition metals. Due to the versatility of metal Lewis acids and chiral Brønsted acids, the dual metal-CPA catalysis is bound to stimulate more evolutionary research in the future, especially in the field of radical-involved enantioselective chemistry, which remains largely underdeveloped.

Acknowledgements Financial support from the National Natural Science Foundation of China (Nos 21722203, 21831002, and 21801116) and Shenzhen Nobel Prize Scientists Laboratory Project (C17783101) is greatly appreciated.

References

1. Mlynarski J (ed) (2017) *Chiral Lewis acids in organic synthesis*. Wiley, Weinheim
2. Akiyama T (2007) *Chem Rev* 107:5744–5758
3. Parmar D, Sugiono E, Raja S, Rueping M (2014) *Chem Rev* 114:9047–9153
4. Parmar D, Sugiono E, Raja S, Rueping M (2017) *Chem Rev* 117:10608–10620
5. Maji R, Mallojjala SC, Wheeler SE (2018) *Chem Soc Rev* 47:1142–1158
6. Akiyama T, Itoh J, Yokota K, Fuchibe K (2004) *Angew Chem Int Ed* 43:1566–1568
7. Uraguchi D, Terada M (2004) *J Am Chem Soc* 126:5356–5357
8. Terada M (2008) *Chem Commun* 35:4097–4112
9. Terada M (2010) *Synthesis* 12:1929–1982
10. Masahiro T (2010) *Bull Chem Soc Jpn* 83:101–119
11. Schenker S, Zamfir A, Freund M, Tsogoeva SB (2011) *Eur J Org Chem* 12:2209–2222
12. Stemper J, Isaac K, Duret V, Retailleau P, Voituriez A, Betzer J-F, Marinetti A (2013) *Chem Commun* 49:6084–6086
13. Stemper J, Isaac K, Ghosh N, Lauwick H, Le Duc G, Retailleau P, Voituriez A, Betzer J-F, Marinetti A (2017) *Adv Synth Catal* 359:519–526
14. Stemper J, Isaac K, Pastor J, Frison G, Retailleau P, Voituriez A, Betzer J-F, Marinetti A (2013) *Adv Synth Catal* 355:3613–3624
15. Zhu J-C, Cui D-X, Li Y-D, Jiang R, Chen W-P, Wang P-A (2018) *ChemCatChem* 10:907–919
16. Isaac K, Stemper J, Servajeau V, Retailleau P, Pastor J, Frison G, Kaupmees K, Leito I, Betzer J-F, Marinetti A (2014) *J Org Chem* 79:9639–9646
17. Yang C, Xue X-S, Jin J-L, Li X, Cheng J-P (2013) *J Org Chem* 78:7076–7085
18. Rueping M, Kuenkel A, Atodiresei I (2011) *Chem Soc Rev* 40:4539–4549
19. Chen D-F, Han Z-Y, Zhou X-L, Gong L-Z (2014) *Acc Chem Res* 47:2365–2377
20. Allen AE, MacMillan DWC (2012) *Chem Sci* 3:633–658
21. Du Z, Shao Z (2013) *Chem Soc Rev* 42:1337–1378
22. Shao Z, Zhang H (2009) *Chem Soc Rev* 38:2745–2755
23. Zhong C, Shi X (2010) *Eur J Org Chem* 16:2999–3025
24. Inamdar SM, Shinde VS, Patil NT (2015) *Org Biomol Chem* 13:8116–8162
25. Yang Z-P, Zhang W, You S-L (2014) *J Org Chem* 79:7785–7798
26. Rueping M, Koenigs RM, Atodiresei I (2010) *Chem Eur J* 16:9350–9365
27. Phipps RJ, Hamilton GL, Toste FD (2012) *Nat Chem* 4:603–614
28. Brak K, Jacobsen EN (2013) *Angew Chem Int Ed* 52:534–561
29. Mayer S, List B (2006) *Angew Chem Int Ed* 45:4193–4195
30. Parra A, Reboredo S, Martín Castro AM, Alemán J (2012) *Org Biomol Chem* 10:5001–5020
31. Mahlau M, List B (2013) *Angew Chem Int Ed* 52:518–533
32. Lv J, Luo S (2013) *Chem Commun* 49:847–858
33. Mukherjee S, List B (2007) *J Am Chem Soc* 129:11336–11337
34. Yan S-Y, Han Y-Q, Yao Q-J, Nie X-L, Liu L, Shi B-F (2018) *Angew Chem Int Ed* 57:9093–9097
35. Lin H-C, Wang P-S, Tao Z-L, Chen Y-G, Han Z-Y, Gong L-Z (2016) *J Am Chem Soc* 138:14354–14361
36. Rueping M, Antonchick AP, Brinkmann C (2007) *Angew Chem Int Ed* 46:6903–6906
37. Terada M, Li F, Toda Y (2014) *Angew Chem Int Ed* 53:235–239
38. Hu W, Xu X, Zhou J, Liu W-J, Huang H, Hu J, Yang L, Gong L-Z (2008) *J Am Chem Soc* 130:7782–7783
39. Jiang J, Xu H-D, Xi J-B, Ren B-Y, Lv F-P, Guo X, Jiang L-Q, Zhang Z-Y, Hu W-H (2011) *J Am Chem Soc* 133:8428–8431
40. Alamsetti SK, Spanka M, Schneider C (2016) *Angew Chem Int Ed* 55:2392–2396
41. Li C, Wang C, Villa-Marcos B, Xiao J (2008) *J Am Chem Soc* 130:14450–14451
42. Miura T, Nishida Y, Morimoto M, Murakami M (2013) *J Am Chem Soc* 135:11497–11500

43. Rong Z-Q, Zhang Y, Chua RHB, Pan H-J, Zhao Y (2015) *J Am Chem Soc* 137:4944–4947
44. Han Z-Y, Xiao H, Chen X-H, Gong L-Z (2009) *J Am Chem Soc* 131:9182–9183
45. Liu X-Y, Che C-M (2009) *Org Lett* 11:4204–4207
46. Muratore ME, Holloway CA, Pilling AW, Storer RI, Trevitt G, Dixon DJ (2009) *J Am Chem Soc* 131:10796–10797
47. Hamilton GL, Kang EJ, Mba M, Toste FD (2007) *Science* 317:496
48. Zbieg JR, Yamaguchi E, McInturff EL, Krische MJ (2012) *Science* 336:324–327
49. Cai Q, Zhao Z-A, You S-L (2009) *Angew Chem Int Ed* 48:7428–7431
50. Sorimachi K, Terada M (2008) *J Am Chem Soc* 130:14452–14453
51. Komanduri V, Krische MJ (2006) *J Am Chem Soc* 128:16448–16449
52. Pellissier H (2019) *Coord Chem Rev* 386:1–31
53. Yu P, Lin J-S, Li L, Zheng S-C, Xiong Y-P, Zhao L-J, Tan B, Liu X-Y (2014) *Angew Chem Int Ed* 53:11890–11894
54. Rauniar V, Wang ZJ, Burks HE, Toste FD (2011) *J Am Chem Soc* 133:8486–8489
55. Ren L, Lei T, Ye J-X, Gong L-Z (2012) *Angew Chem Int Ed* 51:771–774
56. Chen L, Zhang L, Lv J, Cheng J-P, Luo S (2012) *Chem Eur J* 18:8891–8895
57. Mori K, Isogai R, Kamei Y, Yamanaka M, Akiyama T (2018) *J Am Chem Soc* 140:6203–6207
58. Hatano M, Moriyama K, Maki T, Ishihara K (2010) *Angew Chem Int Ed* 49:3823–3826
59. Alix A, Lalli C, Retailleau P, Masson G (2012) *J Am Chem Soc* 134:10389–10392
60. Domžalska A, Ulikowski A, Furman B (2017) Alkaline earth metal based chiral lewis acids. In: Mlynarski J (ed) *Chiral Lewis acids in organic synthesis*. Wiley-VCH, Weinheim, pp 1–23 <https://doi.org/10.1002/9783527802142.ch1>
61. Lv J, Zhang L, Luo S, Cheng J-P (2013) *Angew Chem Int Ed* 52:9786–9790
62. Wang L, Lv J, Zhang L, Luo S (2017) *Angew Chem Int Ed* 56:10867–10871
63. Chirik P, Morris R (eds) (2015) Special Issue: Earth abundant metals in homogeneous catalysis. *Acc Chem Res* 48:(whole issue)
64. Egorova KS, Ananikov VP (2016) *Angew Chem Int Ed* 55:12150–12162
65. Alig L, Fritz M, Schneider S (2019) *Chem Rev* 119:2681–2751
66. Crossley SWM, Obradors C, Martínez RM, Shenvi RA (2016) *Chem Rev* 116:8912–9000
67. Pellissier H, Clavier H (2014) *Chem Rev* 114:2775–2823
68. Bauer I, Knölker H-J (2015) *Chem Rev* 115:3170–3387
69. Tzouras NV, Stamatopoulos IK, Papastavrou AT, Liori AA, Vougioukalakis GC (2017) *Coord Chem Rev* 343:25–138
70. Chirik P, Morris R (2015) *Acc Chem Res* 48:2495
71. Choi J, Fu GC (2017) *Science* 356:7230–7239
72. Wang F, Chen P, Liu G (2018) *Acc Chem Res* 51:2036–2046
73. Kainz QM, Matier CD, Bartoszewicz A, Zultanski SL, Peters JC, Fu GC (2016) *Science* 351:681
74. Fischer C, Fu GC (2005) *J Am Chem Soc* 127:4594–4595
75. Son S, Fu GC (2008) *J Am Chem Soc* 130:2756–2757
76. Schley ND, Fu GC (2014) *J Am Chem Soc* 136:16588–16593
77. Tasker SZ, Standley EA, Jamison TF (2014) *Nature* 509:299
78. Liao S, List B (2010) *Angew Chem Int Ed* 49:628–631
79. McGarrigle EM, Gilheany DG (2005) *Chem Rev* 105:1563–1602
80. Merten C, Pollok CH, Liao S, List B (2015) *Angew Chem Int Ed* 54:8841–8845
81. Gebauer K, Reuß F, Spanka M, Schneider C (2017) *Org Lett* 19:4588–4591
82. El-Sepelgy O, Haseloff S, Alamsetti SK, Schneider C (2014) *Angew Chem Int Ed* 53:7923–7927
83. Chen X, Jiang H, Hou B, Gong W, Liu Y, Cui Y (2017) *J Am Chem Soc* 139:13476–13482
84. Liao S, List B (2012) *Adv Synth Catal* 354:2363–2367
85. Narute S, Parnes R, Toste FD, Pappo D (2016) *J Am Chem Soc* 138:16553–16560
86. Narute S, Pappo D (2017) *Org Lett* 19:2917–2920
87. Morris RH (2016) *Chem Rev* 116:8588–8654
88. Zhang Z, Butt NA, Zhou M, Liu D, Zhang W (2018) *Chin J Chem* 36:443–454
89. Quintard A, Rodriguez J (2014) *Angew Chem Int Ed* 53:4044–4055
90. Zhou S, Fleischer S, Junge K, Beller M (2011) *Angew Chem Int Ed* 50:5120–5124
91. Zhou S, Fleischer S, Jiao H, Junge K, Beller M (2014) *Adv Synth Catal* 356:3451–3455
92. Fleischer S, Werkmeister S, Zhou S, Junge K, Beller M (2012) *Chem Eur J* 18:9005–9010
93. Fleischer S, Zhou S, Werkmeister S, Junge K, Beller M (2013) *Chem Eur J* 19:4997–5003
94. Hopmann KH (2015) *Chem Eur J* 21:10020–10030
95. Lu L-Q, Li Y, Junge K, Beller M (2015) *J Am Chem Soc* 137:2763–2768

96. Yang L, Zhu Q, Guo S, Qian B, Xia C, Huang H (2010) *Chem Eur J* 16:1638–1645
97. Lv J, Zhong X, Luo S (2014) *Chem Eur J* 20:8293–8296
98. Zhang L, Zhang J, Ma J, Cheng D-J, Tan B (2017) *J Am Chem Soc* 139:1714–1717
99. Lalli C, van de Weghe P (2014) *Chem Commun* 50:7495–7498
100. Breugst M, Grée R, Houk KN (2013) *J Org Chem* 78:9892–9897
101. Tsui GC, Liu L, List B (2015) *Angew Chem Int Ed* 54:7703–7706
102. Saito K, Kajiwara Y, Akiyama T (2013) *Angew Chem Int Ed* 52:13284–13288
103. Yazaki R, Kumagai N, Shibasaki M (2010) *J Am Chem Soc* 132:10275–10277
104. Yazaki R, Kumagai N, Shibasaki M (2011) *Chem Asian J* 6:1778–1790
105. Yazaki R, Kumagai N, Shibasaki M (2011) *Org Lett* 13:952–955
106. Zhu Y, Cornwall RG, Du H, Zhao B, Shi Y (2014) *Acc Chem Res* 47:3665–3678
107. Zhao B, Du H, Shi Y (2009) *J Org Chem* 74:8392–8395
108. Zhao B, Peng X, Cui S, Shi Y (2010) *J Am Chem Soc* 132:11009–11011
109. Zhao B, Peng X, Zhu Y, Ramirez TA, Cornwall RG, Shi Y (2011) *J Am Chem Soc* 133:20890–20900
110. Plesniak MP, Huang H-M, Procter DJ (2017) *Nat Rev Chem* 1:77–92
111. Miyabe H, Kawashima A, Yoshioka E, Kohtani S (2017) *Chem Eur J* 23:6225–6236
112. Sibi MP, Manyem S, Zimmerman J (2003) *Chem Rev* 103:3263–3296
113. Tian Y, Chen S, Gu Q-S, Lin J-S, Liu X-Y (2018) *Tetrahedron Lett* 59:203–215
114. Li T, Yu P, Du Y-M, Lin J-S, Zhi Y, Liu X-Y (2017) *J Fluor Chem* 203:210–214
115. Lin J-S, Dong X-Y, Li T-T, Jiang N-C, Tan B, Liu X-Y (2016) *J Am Chem Soc* 138:9357–9360
116. Lin J-S, Wang F-L, Dong X-Y, He W-W, Yuan Y, Chen S, Liu X-Y (2017) *Nat Commun* 8:14841–14851
117. Wang F-L, Dong X-Y, Lin J-S, Zeng Y, Jiao G-Y, Gu Q-S, Guo X-Q, Ma C-L, Liu X-Y (2017) *Chem* 3:979–990
118. Li X-F, Lin J-S, Wang J, Li Z-L, Gu Q-S, Liu X-Y (2018) *Acta Chim Sin* 76:878–882
119. Zeng Y, Liu X-D, Guo X-Q, Gu Q-S, Li Z-L, Chang X-Y, Liu X-Y (2019) *Sci China Chem*. <https://doi.org/10.1007/s11426-019-9528-2>
120. Cheng Y-F, Dong X-Y, Gu Q-S, Yu Z-L, Liu X-Y (2017) *Angew Chem Int Ed* 56:8883–8886
121. Lin J-S, Li T-T, Liu J-R, Jiao G-Y, Gu Q-S, Cheng J-T, Guo Y-L, Hong X, Liu X-Y (2019) *J Am Chem Soc* 141:1074–1083
122. Incerti-Pradillos CA, Hudson D, Malkov AV (2015) *Asymmetric Catal* 2:45–50
123. Lacasse M-C, Poulard C, Charette AB (2005) *J Am Chem Soc* 127:12440–12441
124. Cornwall RG, Wong OA, Du H, Ramirez TA, Shi Y (2012) *Org Biomol Chem* 10:5498–5513
125. Zheng Y, Zhang J (2010) *Adv Synth Catal* 352:1810–1817
126. Voituriezh A, Charette AB (2006) *Adv Synth Catal* 348:2363–2370
127. Voituriezh A, Zimmer LE, Charette AB (2010) *J Org Chem* 75:1244–1250
128. Fuchs M, Schober M, Orthaber A, Faber K (2013) *Adv Synth Catal* 355:2499–2505
129. Wang G-P, Chen M-Q, Zhu S-F, Zhou Q-L (2017) *Chem Sci* 8:7197–7202
130. Furuno H, Hanamoto T, Sugimoto Y, Inanaga J (2000) *Org Lett* 2:49–52
131. Furuno H, Kambara T, Tanaka Y, Hanamoto T, Kagawa T, Inanaga J (2003) *Tetrahedron Lett* 44:6129–6132
132. Furuno H, Hayano T, Kambara T, Sugimoto Y, Hanamoto T, Tanaka Y, Jin YZ, Kagawa T, Inanaga J (2003) *Tetrahedron* 59:10509–10523
133. Jin XL, Sugihara H, Daikai K, Tateishi H, Jin YZ, Furuno H, Inanaga J (2002) *Tetrahedron* 58:8321–8329
134. Jin XL, Sugihara H, Daikai K, Tateishi H, Jin YZ, Furuno H, Inanaga J (2003) *Tetrahedron* 59:877
135. Sugihara H, Daikai K, Jin XL, Furuno H, Inanaga J (2002) *Tetrahedron Lett* 43:2735–2739
136. Suzuki S, Furuno H, Yokoyama Y, Inanaga J (2006) *Tetrahedron Asymmetry* 17:504–507
137. Liu C, Lv J, Luo S, Cheng J-P (2014) *Org Lett* 16:5458–5461
138. Jeong HJ, Kim DY (2018) *Org Lett* 20:2944–2947
139. Gualandi A, Rodeghiero G, Cozzi PG (2018) *Asian J Org Chem* 7:1957–1981
140. Terada M, Ota Y, Li F, Toda Y, Kondoh A (2016) *J Am Chem Soc* 138:11038–11043
141. Ota Y, Kondoh A, Terada M (2018) *Angew Chem Int Ed* 57:13917–13921
142. Terada M, Toda Y (2009) *J Am Chem Soc* 131:6354–6355
143. Terada M, Komuro T, Toda Y, Korenaga T (2014) *J Am Chem Soc* 136:7044–7057